Article

Microbial Genetic Composition Tunes Host Longevity

Graphical Abstract

Highlights

- Systematic analysis of longevity-promoting microbial genetic variations

- Colanic acid as a pro-longevity natural compound effective in different species

- Bacterial metabolites regulate host mitochondrial dynamics and UPR^{mit}
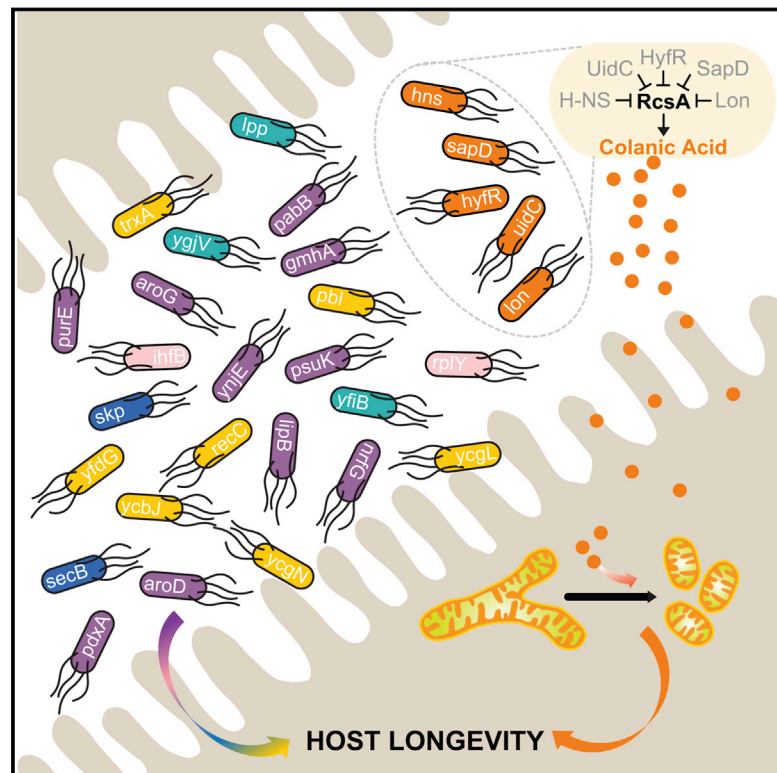
Authors

Bing Han, Priya Sivaramakrishnan, Chih-Chun J. Lin, ..., Jin Wang, Christophe Herman, Meng C. Wang

Correspondence

wmeng@bcm.edu

In Brief

The genetic composition of gut microbes controls the production of metabolites that impact host longevity.

CrossMark

CellPress

Article

Microbial Genetic Composition Tunes Host Longevity

Bing Han,[1,2] Priya Sivaramakrishnan,[2] Chih-Chun J. Lin,[1,2] Isaiah A.A. Neve,[1,2] Jingquan He,[3] Li Wei Rachel Tay,[3] Jessica N. Sowa,[1,2] Antons Sizovs,[4] Guangwei Du,[3] Jin Wang,[4] Christophe Herman,[2,5] and Meng C. Wang[1,2,5,6,*]

[1]Huffington Center on Aging, Baylor College of Medicine, Houston, TX 77030, USA
[2]Department of Molecular and Human Genetics, Baylor College of Medicine, Houston, TX 77030, USA
[3]Department of Integrative Biology and Pharmacology, University of Texas Health Science Center at Houston, Houston, TX 77030, USA
[4]Department of Pharmacology, Baylor College of Medicine, Houston, TX 77030, USA
[5]Dan L. Duncan Comprehensive Cancer Center, Baylor College of Medicine, Houston, TX 77030, USA
[6]Lead Contact
*Correspondence: wmeng@bcm.edu
http://dx.doi.org/10.1016/j.cell.2017.05.036

SUMMARY

Homeostasis of the gut microbiota critically influences host health and aging. Developing genetically engineered probiotics holds great promise as a new therapeutic paradigm to promote healthy aging. Here, through screening 3,983 *Escherichia coli* mutants, we discovered that 29 bacterial genes, when deleted, increase longevity in the host *Caenorhabditis elegans*. A dozen of these bacterial mutants also protect the host from age-related progression of tumor growth and amyloid-beta accumulation. Mechanistically, we discovered that five bacterial mutants promote longevity through increased secretion of the polysaccharide colanic acid (CA), which regulates mitochondrial dynamics and unfolded protein response (UPR^{mt}) in the host. Purified CA polymers are sufficient to promote longevity via ATFS-1, the host UPR^{mt}-responsive transcription factor. Furthermore, the mitochondrial changes and longevity effects induced by CA are conserved across different species. Together, our results identified molecular targets for developing pro-longevity microbes and a bacterial metabolite acting on host mitochondria to promote longevity.

INTRODUCTION

In large part, because of progress in curing infectious and contagious diseases, modern society is progressively aging and is made up of an ever-growing proportion of elderly individuals. Improving healthy aging and preventing aging-associated chronic disabilities have become a priority of current biomedical research. Although our understanding of aging has been deepened by discoveries of several conserved molecular mechanisms (Kenyon, 2010), few longevity-promoting compounds have been discovered to date (Cabreiro et al., 2013; Harrison et al., 2009, 2014; Howitz et al., 2003).

A growing body of evidence suggests that gut microbiota—diverse microorganisms inhabiting the digestive track—are tightly linked to the aging process of their host (Cho and Blaser, 2012; Heintz and Mair, 2014). This community of microbial species, among which bacteria are predominant and most extensively studied, not only generates metabolites essential for various host functions (Lee and Hase, 2014) but also mediates effects of exogenous chemicals on the animals they reside in (Cabreiro et al., 2013). Changes in the bacterial composition of the microbiota have been observed in elderly people, and diet-driven microbiota alterations have been shown to improve their health (Claesson et al., 2012; Yatsunenko et al., 2012). However, most of our knowledge on microbiota is limited to taxonomic and metagenomic profiling, whereas functions of individual microbial genes and their molecular mechanisms in modulating host aging remain elusive. This is due in part to the high complexity of mammalian gut microbiota and to technical challenges of isolating specific pro-longevity microbial variations.

The nematode *Caenorhabditis elegans* with its short and easily monitored lifespan as well as defined microbiota, is a powerful model for disentangling the interactions between microbes and host aging (Heintz and Mair, 2014). Under standard laboratory conditions, *C. elegans* are reared on a single bacterial strain of *Escherichia coli*. Starting from early adulthood of the nematodes, bacterial cells colonize the intestinal lumen and form their entire gut microbiota (Clark and Hodgkin, 2014). Using this simple model system, studies have demonstrated the crucial role that the microbiota play in regulating host longevity (Garigan et al., 2002; Portal-Celhay et al., 2012). Some bacterial variants have been serendipitously identified as determinants of host lifespan (Larsen and Clarke, 2002; Virk et al., 2012), and small molecules secreted from bacteria, such as certain non-coding RNAs and nitric oxide, have been linked to host longevity in the context of specific bacterial backgrounds (Gusarov et al., 2013; Liu et al., 2012). However, a systematic analysis on the longevity-related effects of bacterial genetic factors has not been performed.

In this study, we designed a high-throughput screening platform to identify microbial pro-longevity factors from the entire collection of *E. coli* non-essential gene deletion mutants (Baba et al., 2006). We discovered a series of microbial genetic factors that regulate host health and longevity and demonstrated their interactions with several known aging-regulatory pathways of the host. We also discovered a probiotic mechanism distinct from these known pathways, which functions through induction of a secreted polysaccharide that promotes host longevity by

A

Category	Gene	Description	Lifespan Extension	*E. coli* BW25113	*E. coli* MG1655	Adult Effect
Transcription &Translation	*hns*	global DNA-binding transcriptional dual regulator	40%	Y	Y	Y
	ihfB	integration host factor; DNA-binding protein	35%	Y	Y	Y
	hyfR	DNA-binding transcriptional activator	16%	Y	Y	Y
	rplY	50S ribosomal subunit protein	11%	Y	Y	N
Metabolism & Respiration	*aroG*	3-deoxy-D-arabino-heptulosonate-7-phosphate synthase	29%	Y	Y	Y
	aroD	3-dehydroquinate dehydratase	24%	Y	Y	N
	lipB	lipoyl-protein ligase	23%	Y	Y	Y
	purE	N5-carboxyaminoimidazole ribonucleotide mutase	21%	Y	Y	Y
	pdxA	4-hydroxy-L-threonine phosphate dehydrogenase	21%	Y	Y	Y
	*gmhA**	D-sedoheptulose 7-phosphate isomerase	19%	Y	N/A	N/A
	pabB	aminodeoxychorismate synthase	18%	Y	Y	N
	ynjE	thiosulfate sulfur transferase	18%	Y	Y	Y
	nrfG	heme lyase	17%	Y	Y	Y
	psuK	pseudouridine kinase	10%	Y	N	N
Membrane & Transport	*lpp*	murein lipoprotein	27%	Y	Y	Y
	yfiB	outer membrane lipoprotein	20%	Y	N	N
	sapD	antimicrobial peptide transporter	17%	Y	Y	Y
	uidC	outer membrane porin protein	17%	Y	N	Y
	ygjV	inner membrane protein	12%	Y	Y	Y
Protease & Chaperone	*secB*	protein export chaperone	29%	Y	Y	Y
	lon	DNA-binding ATP-dependent protease	25%	Y	Y	Y
	skp	periplasmic chaperone	16%	Y	Y	Y
Others	*pbl*	lytic transglycosylase	21%	Y	N	N
	ycbJ	unknown	19%	Y	Y	Y
	trxA	thioredoxin	15%	Y	Y	Y
	ycgL	unknown	14%	Y	Y	N
	ycgN	unknown	12%	Y	N	Y
	recC	exonuclease V	11%	Y	Y	Y
	yfdG	prophage; bactoprenol-linked glucose translocase	10%	Y	Y	Y
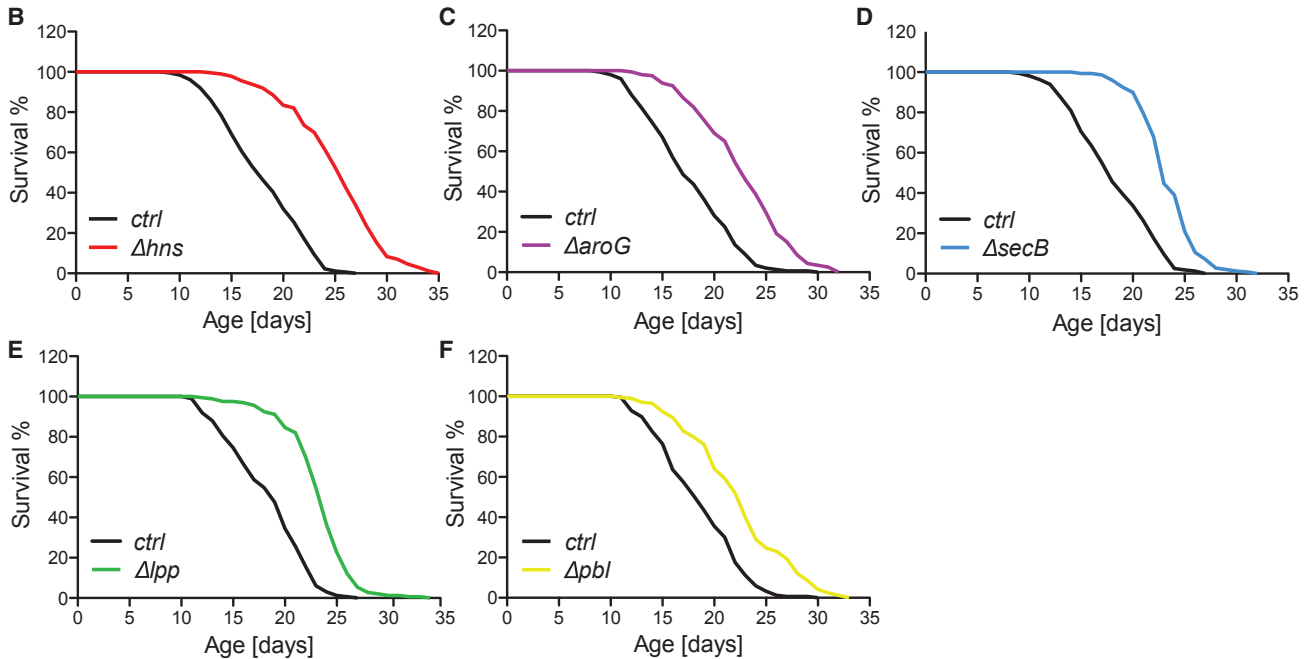
(legend on next page)

tuning mitochondrial homeostasis. Our data thus reveal the crucial link between microbiota genetic composition and host longevity, provide a roadmap for developing genetically engineered pro-longevity probiotics, and uncover a chemical dialog between bacteria and mitochondria.

RESULTS

Genome-wide Analysis of Microbial Factors Regulating Host Longevity

To systematically identify microbial factors that promote host longevity, we conducted a genome-wide screen of the *E. coli* single-gene knockout library for lifespan extension in *C. elegans*. We used the parental strain of this library, *E. coli* K-12 BW25113, as an experimental control. *C. elegans* grown on this control bacteria show similar development, reproduction, and lifespan as those on standard laboratory *E. coli* strains (Figures S1A–S1C). Because of the crucial role of the reproductive system in regulating *C. elegans* longevity, we applied a high-throughput screening strategy different from the conventional method that interrupts reproduction. We selected the *sqt-3(e2117)* collagen mutant of *C. elegans* that reproduces normally but is embryonically lethal at 25°C (Wang et al., 2014). Using this mutant, we performed the primary screen at the restrictive temperature to avoid labor-intensive animal transfer without interrupting normal reproduction (Figures S1D and S1E).

Out of the 3,983 *E. coli* mutants, 68 prolonged lifespan in the *sqt-3* background (Table S1). We next validated the longevity effects of these 68 *E. coli* mutants in wild-type *C. elegans* at 20°C and identified 35 bacterial mutants that significantly prolonged host lifespan by more than 10% (p < 0.001, Table S2). To determine whether the longevity effects of these bacterial mutants are indeed conferred by the deletion of their annotated genes, we reintroduced these mutations into the parental strain BW25113 and confirmed the lifespan-extending effects of 29 bacterial mutants (Figure 1A; Table S3). These longevity-promoting bacterial mutants appear functionally heterogeneous, and deletions of genes in different functional groups can lead to comparable levels of lifespan extension in *C. elegans* (Figures 1B–1F). Moreover, 21 of these bacterial mutants preserved their longevity effects when only provided during adulthood of *C. elegans* (Figure 1A; Table S3). We also introduced these mutations into a wild-type *E. coli* strain, MG1655, and showed that 23 of them significantly prolong *C. elegans* lifespan (Figure 1A; Table S3). Together, these results show that alterations in bacterial genetic composition can modulate the aging process of the host, and these effects are not restricted to specific microbial backgrounds or host developmental stages.

In order to rule out the possibility that increased lifespan is caused by differences in bacterial amount, we ensured the same numbers of bacteria supplied to the worms based on both light-scattering measurements and cell counting by microscopy. We also measured viability of the identified longevity-promoting bacterial mutants, showing that the numbers of live bacterial cells initially provided to the worms are similar (Figure S2A). When comparing host colonization capacities among these bacteria, we observed a decrease in five mutants and an increase in two mutants (Figures S2B and S2C). Therefore, there is no direct association between the viability or the host colonization of the bacterial mutants and their lifespan-extending effects.

Microbial Factors Ameliorate Age-Related Pathologies of Tumor Progression and Amyloid-β Accumulation

Advanced age is a major risk factor for various chronic diseases, such as cancer and neurodegeneration (Niccoli and Partridge, 2012). Next, we tested whether bacterial mutants identified in our screen could increase the survival of host animals under age-associated pathological conditions. In the *C. elegans* *glp-1(ar202)* mutant, excessive proliferation of germ cells results in germline tumors that migrate into somatic tissues and causes early death (Pepper et al., 2003). We found that 16 bacterial mutants increase the survival rate of the *glp-1(ar202)* mutant (Figure 2A; Table S4).

In addition, *C. elegans* transgenic strains expressing toxic human amyloid-β (Aβ) exhibit early decline in physical activities and shortened lifespan (Link, 1995). Among the 29 lifespan-extending bacterial mutants, we identified 14 that significantly prolong the lifespan of the Aβ transgenic strains (Figure 2B; Table S5) and 12 of them substantially delay age-associated paralysis (Figure 2C). Altogether, we discovered 13 bacterial mutants that protect *C. elegans* from lethality of both germline tumors and Aβ accumulation (Figure 2D), suggesting they may improve the overall fitness of the host.

Interaction of Beneficial Microbial Factors with Host Longevity Mechanisms

To gain insight into the molecular mechanisms mediating the beneficial effects of these bacterial mutants, we examined whether they act through several known longevity mechanisms in the host, including the insulin/insulin-like growth factor (IGF)-1 and the target of rapamycin (TOR) signaling pathways as well as caloric restriction (CR). The FoxO transcription factor DAF-16 is a necessary downstream mediator of insulin/IGF-1

Figure 1. Bacterial Mutants Promote Host Longevity

(A) A genome-wide screen of the *E. coli* BW25113 single-gene knockout library identified 29 mutants that prolong *C. elegans* lifespan by >10% (p < 0.001, log rank test). Twenty-one of these mutants significantly prolong lifespan when provided only to *C. elegans* adults (p < 0.05, log rank test) and 23 of them also promote host longevity in the wild-type *E. coli* MG1655 strain background (p < 0.05, log rank test). These longevity-promoting bacterial mutants are classified into different functional categories, delineated by different colors. An asterisk marks the *gmhA* gene, when deleted, resulting in resistance to P1 phage.

(B–F) Lifespan extensions by different functional categories of bacterial mutants are represented by *Δhns* (B), *ΔaroG* (C), *ΔsecB* (D), *Δlpp* (E), and *Δpbl* (F), respectively.

See Figure S1 for information on the control bacteria and the design of the screen, Figure S2 for information of viability and colonization capacities of the mutants, Figure S7 for the enrichment of genes involved in chorismate metabolism, and Tables S1–S3 for lifespan data including animal numbers, mean and median lifespans, and statistics.
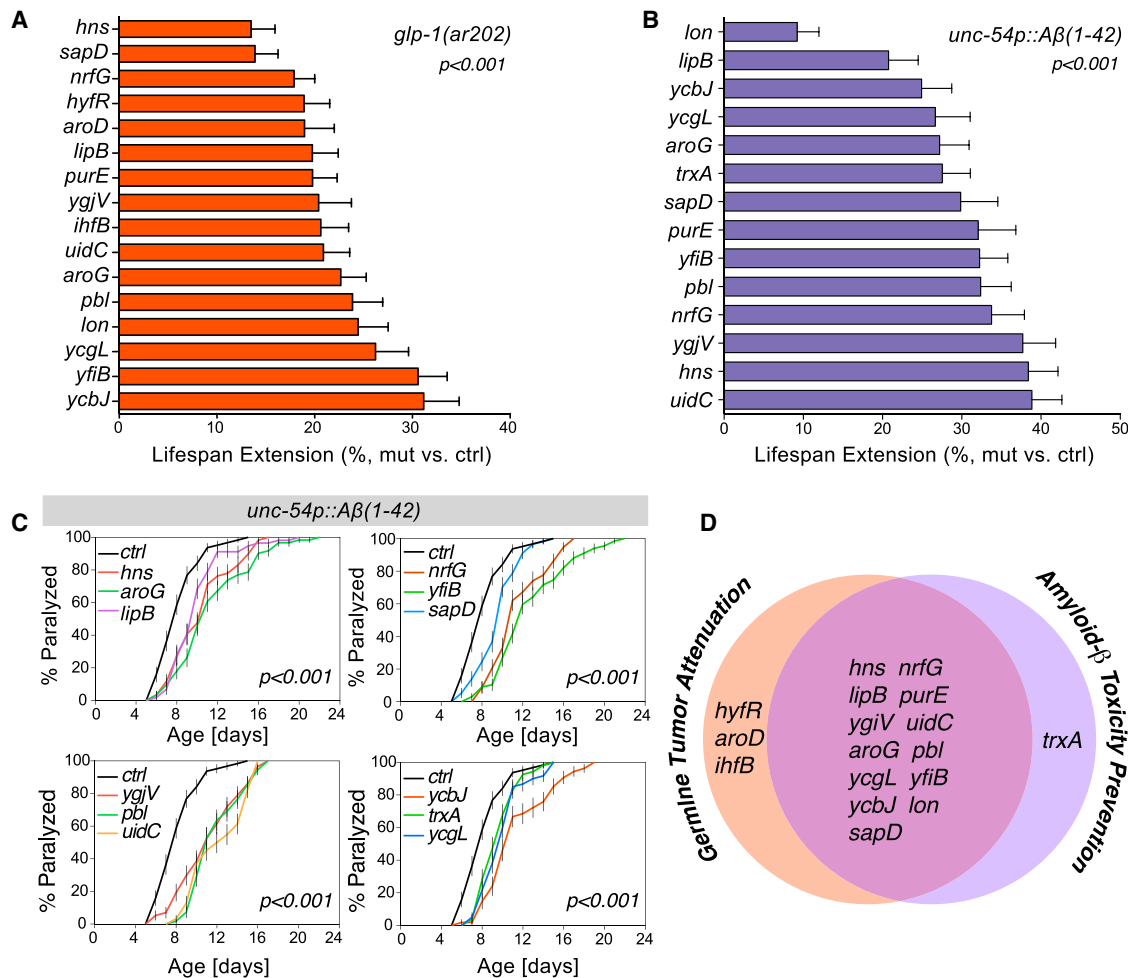
Figure 2. Bacterial Mutants Attenuate Age-Related Pathologies in the Host

(A) Sixteen bacterial mutants significantly increase the survival of the *C. elegans glp-1(ar202)* mutants, which exhibit early death due to age-related progression of germline tumors (p < 0.001, log rank test).

(B) Ectopic expression of human amyloid-β (Aβ) in the *C. elegans* CL2006 transgenic strain *dvls2[unc-54p::Aβ(1-42)]* leads to a shortened lifespan. Fourteen bacterial mutants significantly increase the survival of this strain (p < 0.001, log rank test). Survival analyses were conducted three times independently. The average percentage of lifespan extension by each bacterial mutant versus the parental control is shown, and error bars represent SEM.

(C) Twelve of the bacterial mutants that increase the survival of the CL2006 strain also significantly delay the onset of paralysis caused by Aβ proteotoxicity (p < 0.001, log rank test). Error bars represent SEM.

(D) The sets of the bacterial mutants that protect *C. elegans* against the lethality of germline tumor and Aβ accumulation are largely overlapped.

See Tables S4 and S5 for survival data of three independent trails including animal numbers, mean lifespans, and statistics.

and c-Jun N-terminal kinase (JNK) longevity signaling pathways (Lin et al., 1997; Ogg et al., 1997; Oh et al., 2005; Wang et al., 2005). RSKS-1, the ribosomal protein S6 kinase and RAGA-1, the Ras-related GTPase are crucial regulators of the TOR complex 1 longevity mechanism (Pan et al., 2007; Robida-Stubbs et al., 2012; Stanfel et al., 2009). RICT-1, a subunit of the TOR complex 2, is also involved in regulating the lifespan of *C. elegans* (Mizunuma et al., 2014; Soukas et al., 2009). We investigated the lifespan of the *daf-16(mgDf47)*, *rsks-1(ok1255)*, *raga-1(ok386)*, and *rict-1(ft7) C. elegans* mutants grown on each bacterial mutant to determine whether these host factors contribute to the longevity effects of the bacterial mutants. Out of the 29 bacterial mutants, there are 7, 13, 11, and 19 mutants

unable to significantly prolong the lifespan of the *C. elegans daf-16*, *rsks-1*, *raga-1*, and *rict-1* mutants, respectively (p > 0.05, Figure 3), suggesting that they act through the host insulin/IGF-1 and/or TOR signaling pathway to regulate longevity.

CR is an extensively studied intervention that promotes longevity in a variety of species (Fontana et al., 2010). We further examined whether CR plays a role in mediating the longevity effects of these bacterial mutants. We first assessed the effects of the bacterial mutants on feeding and defecation behaviors of wild-type *C. elegans.* When providing similar amounts of bacteria (Figure S2A), we found that only two bacterial mutants lowered the pharyngeal pumping rate (Figure S3A) and another two slowed down defecation (Figure S3B), suggesting minimal

Mutant	daf-16(mgDf47)			rsks-1(ok1255)			raga-1(ok386)			rict-1(ft7)			eat-2(ad465)		
	Total N (censor N)	Lifespan extension	p value	Total N (censor N)	Lifespan extension	p value	Total N (censor N)	Lifespan extension	p value	Total N (censor N)	Lifespan extension	p value	Total N (censor N)	Lifespan extension	p value
lon	167 (11)	22%	<0.001	102(1)	25%	<0.001	107(5)	12%	<0.001	133 (16)	10%	0.015	189 (3)	36%	<0.001
hns	155 (13)	17%	<0.001	101(2)	19%	<0.001	86(7)	6%	0.001	123 (8)	29%	<0.001	178 (8)	46%	<0.001
ihfB	212 (8)	29%	<0.001	123(3)	19%	<0.001	78(0)	19%	<0.001	118 (22)	-1%	0.612	178 (3)	48%	<0.001
aroD	186 (7)	20%	<0.001	102(0)	29%	<0.001	124(0)	25%	<0.001	119 (13)	-5%	0.486	159 (8)	43%	<0.001
secB	161 (10)	15%	<0.001	104(0)	28%	<0.001	115(1)	15%	<0.001	121 (10)	4%	0.098	158 (8)	54%	<0.001
gmhA	191 (6)	13%	<0.001	113(0)	14%	0.004	84(0)	31%	<0.001	95 (7)	1%	0.671	194 (2)	31%	<0.001
ycgL	187 (9)	15%	<0.001	94(1)	6%	0.054	102(0)	10%	<0.001	99 (12)	6%	0.079	189 (12)	14%	<0.001
hyfR	227 (10)	17%	<0.001	94(2)	9%	0.099	76(1)	-1%	0.250	101 (8)	10%	0.003	166 (11)	27%	<0.001
uidC	165 (14)	15%	<0.001	100(0)	-1%	0.170	121(0)	-11%	<0.001	138 (12)	18%	<0.001	155 (11)	18%	<0.001
sapD	209 (5)	11%	<0.001	106(0)	5%	0.569	120(0)	3%	0.171	128 (9)	14%	<0.001	181 (11)	18%	<0.001
ycbJ	173 (1)	21%	<0.001	111(6)	-9%	0.007	102(0)	2%	0.206	121 (13)	16%	<0.001	186 (0)	8%	0.002
yfiB	219 (12)	17%	<0.001	94(0)	6%	0.536	84(0)	1%	0.582	109 (10)	8%	0.052	174 (0)	20%	<0.001
ygjV	180 (4)	14%	<0.001	90(0)	1%	0.251	89(0)	4%	0.387	106 (8)	0%	0.813	208 (5)	10%	<0.001
purE	151 (15)	10%	<0.001	108(0)	2%	0.671	72(2)	5%	0.075	113 (9)	5%	0.174	178 (14)	13%	<0.001
nrfG	218 (11)	10%	0.001	121(1)	3%	0.960	111(0)	4%	0.275	106 (5)	1%	0.711	190 (6)	14%	<0.001
aroG	193 (5)	19%	<0.001	102(0)	1%	0.804	94(0)	1%	0.494	118 (3)	7%	0.088	173 (10)	8%	0.005
pbl	204 (2)	19%	<0.001	126(0)	5%	0.725	104(0)	1%	0.343	113 (18)	-10%	0.021	151 (4)	3%	0.381
lpp	180 (6)	5%	0.008	123(5)	14%	0.033	122(3)	18%	<0.001	105 (8)	8%	0.031	205 (1)	36%	<0.001
pdxA	187 (10)	6%	0.003	107(1)	19%	0.001	88(1)	15%	<0.001	102 (17)	9%	0.009	169 (7)	14%	<0.001
lipB	158 (12)	8%	0.001	108(0)	18%	<0.001	115(4)	24%	<0.001	127 (6)	0%	0.891	185 (10)	30%	<0.001
ynjE	203 (13)	5%	0.022	94(0)	26%	<0.001	84(3)	10%	0.003	113 (11)	-9%	0.016	198 (9)	19%	<0.001
pabB	172 (4)	8%	<0.001	116(3)	11%	0.043	105(0)	20%	<0.001	138 (14)	-6%	0.217	161 (5)	19%	<0.001
trxA	159 (15)	1%	0.419	114(2)	11%	0.043	107(2)	10%	0.003	122 (13)	11%	0.007	186 (16)	18%	<0.001
recC	150 (12)	4%	0.293	133(2)	14%	0.016	93(0)	11%	0.006	130 (17)	14%	<0.001	161 (9)	4%	0.037
skp	167 (9)	4%	0.057	104(0)	20%	<0.001	110(1)	13%	<0.001	124 (15)	-4%	0.355	154 (15)	33%	<0.001
rplY	163 (7)	4%	0.094	118(0)	11%	0.042	99(3)	13%	<0.001	105 (8)	-11%	0.008	189 (2)	-8%	0.011
yfdG	161 (9)	3%	0.235	80(1)	12%	0.048	101(2)	7%	<0.001	114 (10)	1%	0.792	177 (12)	24%	<0.001
ycgN	157 (13)	4%	0.036	95(2)	-3%	0.155	127(3)	7%	0.015	111 (5)	7%	0.169	167 (3)	11%	<0.001
psuK	208 (13)	2%	0.358	97(3)	7%	0.222	96(0)	3%	0.438	101 (11)	3%	0.286	177 (8)	-7%	0.015

- Lifespan extension ≥ 10%, p<0.05
- Lifespan extension 5%~10%, p<0.05
- Lifespan extension <5%, p>0.05

Figure 3. Genetic Interaction Analyses with Host Longevity Mechanisms

Bacterial mutants were examined for their effects on the lifespans of the daf-16(mgDf47), rsks-1(ok1255), raga-1(ok386), rict-1(ft7), and eat-2(ad465) C. elegans mutants. Grey colors mark the candidates showing dependence on these known host longevity regulatory pathways, and apricot colors mark the ones acting independently. Total N, the number of total animals; censor N, the number of censored animals; Lifespan extension, the percentage of lifespan extension in different C. elegans mutants on each bacterial mutant compared to those on parental control bacteria; p values, bacterial mutant versus parental control by log rank test.

See Figure S3 for effects of bacterial mutants on C. elegans feeding and defecation behaviors.

involvement of low food intake in most bacteria-induced longevity effects.

In addition, CR can be genetically mimicked using C. elegans eat-2 mutants that have defective pharyngeal contraction during feeding (Lakowski and Hekimi, 1998). We examined how the bacterial mutants affect the host lifespan under this genetically mimicked CR condition. We first confirmed that none of the bacterial mutants alter the pharyngeal contraction rate of the eat-2 mutant (Figure S3C). Next, we found that only 4 out of the 29 bacterial mutants do not significantly prolong the lifespan of the eat-2(ad465) mutant (p > 0.05, Figure 3), suggesting that CR does not contribute to the longevity effects of the other 25 bacterial mutants.

Bacterial Colanic Acid Overproduction as a Longevity-Promoting Mechanism

The genetic interaction analyses between longevity-promoting bacterial mutations and host mutations lead to the discovery of two bacterial mutants, Δhns and Δlon, which act independently of DAF-16, TOR, or CR (Figure 3). Interestingly, both lon and hns genes regulate biosynthesis of colanic acid (CA), a polysaccha-

ride secreted by many enterobacterial species including E. coli K-12 (Figure 4A) (Grant et al., 1969). RcsA, the central activator of the CA biosynthesis gene cluster, is degraded by the ATP-dependent protease Lon (Gottesman et al., 1985; Torres-Cabassa and Gottesman, 1987) and is also repressed by the global transcriptional regulator H-NS (Sledjeski and Gottesman, 1995) (Figure 4A). We thus hypothesized that CA overproduction underlies the longevity promoting effects of these two mutants. To test this hypothesis, we first measured the CA levels in bacterial culture medium and found that CA secretion is elevated in both Δlon and Δhns, compared to the parental control (Figure 4B). Furthermore, we discovered that the ΔrcsA deletion fully suppresses the CA overproduction in these mutants (Figure 4B). The ΔrcsA deletion completely abrogates the lifespan-extending effect of the Δlon mutant, suggesting a full requirement of CA overproduction (Figure 4C; Table S6). For the Δhns mutant, the ΔrcsA deletion exerts a partial suppression, indicating that both CA-dependent and -independent mechanisms contribute to its longevity effect (Figure 4D; Table S6). On the other hand, ΔaroD, a mutant that does not induce CA secretion, acts independently of RcsA to promote longevity (Figure 4E; Table S6)
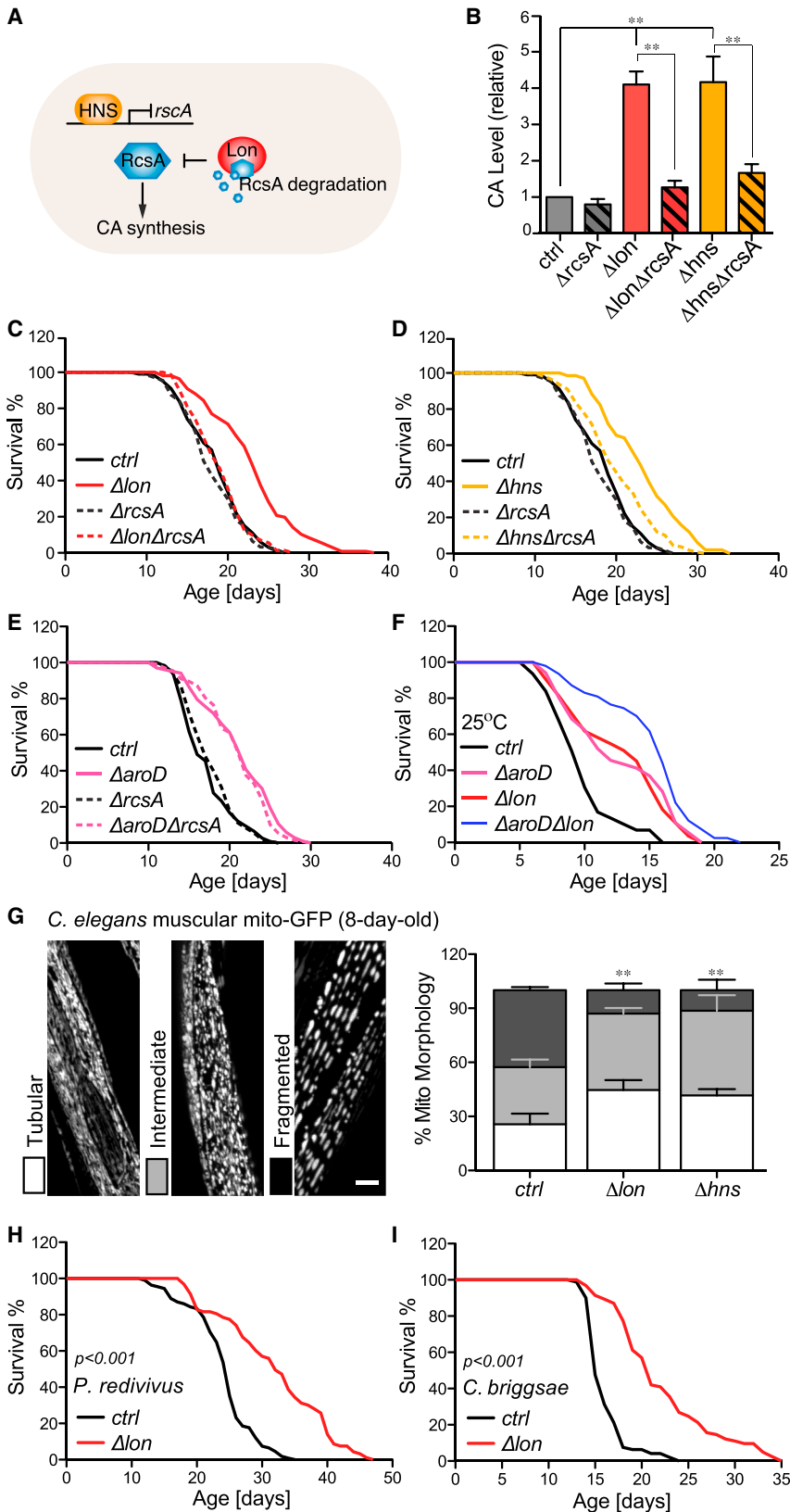
Figure 4. Colanic Acid-Overproducing Bacterial Mutants Promote Host Longevity

(A) Schematic depiction of biosynthesis of colanic acid (CA) in bacteria. RcsA, a positive activator required for CA biosynthesis, can be transcriptionally repressed by H-NS and degraded by the Lon protease.

(B) Both Δ*lon* and Δ*hns* show increased CA secretion in the culture medium, which are completely suppressed by the deletion of *rcsA* (**p < 0.01, one-way ANOVA followed by Bonferroni's multiple comparison test). Error bars represent SEM.

(C and D) The Δ*rcsA* deletion suppresses the lifespan extension conferred by Δ*lon* (C) and Δ*hns* (D) (p < 0.001, double mutants versus corresponding single mutants, log rank test). Experiments were conducted in parallel with same parental controls and Δ*rcsA* mutants.

(E) The Δ*rcsA* deletion does not affect the lifespan extension conferred by Δ*aroD* (p > 0.05, Δ*aroD*Δ*rcsA* versus Δ*aroD*, log rank test).

(F) Δ*lon* further enhances the lifespan extension conferred by Δ*aroD* (p < 0.05, Δ*aroD*Δ*lon* versus Δ*aroD*, log rank test).

(G) Both Δ*lon* and Δ*hns* mutants significantly lower the levels of mitochondrial fragmentation in the transgenic *C. elegans* expressing mito-GFP in body wall muscles (*raxIs[myo-3p::mitoGFP]*), visualized at day 8 adulthood. Different mitochondrial morphologies were classified as tubular, intermediate, and fragmented (representative images are shown; scale bar, 10 μm) and quantified double-blindly. Error bars represent SEM; **p < 0.01 bacterial mutant versus parental control by Student's t test.

(H and I) The Δ*lon* bacterial mutant significantly prolongs the lifespan of *P. redivivus* (H) and *C. briggsae* (I) (p < 0.001, log rank test).

See Figure S4 for information on additional CA-overproducing mutants and Table S6 for lifespan data including animal numbers, mean and median lifespans, and statistics.

and has an additive lifespan-extending effect with Δ*lon* (Figure 4F; Table S6). Interestingly, there are another three bacterial mutants that overproduce CA and extend *C. elegans* lifespan in an RcsA-dependent manner (Figure S4; Table S6). Together, these results suggest CA overproduction as a probiotic mechanism linking microbial metabolism and host longevity.

In addition to prolonging lifespan, these CA-overproducing bacterial mutants improve *C. elegans* tissue maintenance during aging. Mitochondrial dysfunction in body wall muscles is a hallmark of somatic aging, which is associated with increased mitochondrial fragmentation (Regmi et al., 2014). We found that the CA-overproducing bacterial mutants attenuate this age-associated muscular mitochondrial fragmentation (Figures 4G and S4E). We further showed that the lifespan-extending effect of the Δ*lon* mutant is evolutionarily conserved in nematode species that have diverged from *C. elegans* more than 100 million years ago, including *Panagrellus redivivus* (Figure 4H; Table S6) and *C. briggsae* (Figure 4I; Table S6).

Purified CA Sufficiently Promotes Host Longevity
In order to directly evaluate the efficacy of CA in promoting host longevity, we supplemented purified CA to wild-type *C. elegans*. Strikingly, CA supplementation sufficiently prolonged the lifespan of *C. elegans* grown on *E. coli* K-12 BW25113 (Figure 5A; Table S7). CA also extended *C. elegans* lifespan when supplemented together with a diverse range of bacteria, including another *E. coli* K-12 strain, HT115 (Figure 5B; Table S7), and gram-positive *Bacillus subtilis* (Figure 5C; Table S7). In contrast, when supplemented with a commonly used laboratory bacterial strain, *E. coli* OP50, CA lost its lifespan-extending effect (Figure 5D; Table S7). Interestingly, as a B-type *E. coli*, OP50 is naturally *lon*-deficient and produces more CA than the K-12 strain (Figure 5E). When we restored *lon* in OP50, worms exhibited reduced lifespan that was restored upon CA supplementation (Figure 5D; Table S7). These observations on *E. coli* OP50 suggest that microbial *lon* deficiency and dietary CA supplementation are both effective to promote host longevity and act through the same mechanism.

CA supplementation also delayed the onset of muscular mitochondrial fragmentation (Figure 5F) and consequently improved locomotion activities of aged *C. elegans* (Figure 5G) and increased the survival of *C. elegans* carrying germline tumor or toxic human Aβ (Figure 5H). Intriguingly, we found that adult-only dietary supplementation of CA substantially increases the lifespan of wild-type *Drosophila melanogaster* (Figure 5I) and improves their spontaneous activities (Figure 5J), supporting a well-conserved longevity effect of CA across evolutionarily distant hosts.

Direct Impact of CA Polymers on the Host but Not Bacteria
The CA polymer contains a repeating unit of glucose, galactose, fucose, and glucuronic acid, which are further decorated by pyruvate and acetate (Sutherland, 1969) (Figure 6A). After being synthesized in the cytoplasm, CA repeating units are transported to periplasm and linked together by the CA polymerase, WcaD (Stevenson et al., 1996). When we supplemented *C. elegans* with the six monomers of CA, either separately or in combination,

no lifespan extension was detected (Figure S5A). Moreover, neither the Δ*lon*Δ*wcaD* mutant nor extract from this double mutant prolonged *C. elegans* lifespan (Figures 6B and S5B; Tables S6 and S7). Therefore, the monomers or the single repeating units of CA are not sufficient to induce host longevity. Gel permeation chromatography analysis determined that the molecular weight of purified CA is ~3.4 kDa (Figure 6C), suggesting that CA polymers with three or more repeating units are required for their longevity effects. Moreover, supplementation of two other extracellular polysaccharides, hyaluronic acid and alginic acid, did not extend *C. elegans* lifespan (Figure S5C), supporting the specificity of CA as a longevity-promoting polysaccharide.

Next, to test whether CA increases the survival of *C. elegans* by reducing bacterial growth or pathogenicity, we monitored the growth of bacteria treated with CA. Interestingly, instead of inhibiting growth, CA had a slight growth-stimulating effect after the stationary phase (Figure 6D). Furthermore, with CA supplementation, the capacity of bacteria colonized in the *C. elegans* gut was not reduced (Figure 6E). In addition, CA neither attenuated the lethality caused by pathogenic bacteria, *Pseudomonas aeruginosa* and *Enterococcus faecalis* (Figures 6F and 6G), nor affected the expression of several well-known pathogenic responsive genes (Figure 6H). Therefore, the longevity-promoting effect of CA does not result from inhibiting bacterial growth or pathogenicity.

To determine whether live bacteria mediate the beneficial effect of CA on the host, we killed bacteria with ultraviolet radiation or inactivated them with chloramphenicol before CA supplementation. We found that CA remains its lifespan-extending capacity when supplemented with dead bacteria, and the magnitude of lifespan extension is unaffected (Figures 6I and 6J; Table S7). Furthermore, we discovered that host endocytotic genes, *rab-5* and *rab-7* (Grant et al., 2001) are required for CA to prolong lifespan (Figures S5D–S5F; Table S7). Together, these results show that CA alone is sufficient to exert its beneficial effects and requires endocytosis-mediated uptake into host intestinal cells.

CA Acts on Host Mitochondria to Promote Longevity
To further investigate the molecular mechanism underlying the longevity effect of CA, we examined the lifespan of various *C. elegans* mutants raised on the CA-overproducing Δ*lon* bacterial mutant. Similar to the *daf-16*, *rict-1*, *rsks-1*, *raga-1*, and *eat-2* mutants (Figure 3), the hypoxia-inducible factor mutant, *hif-1(ia4)* (Leiser and Kaeberlein, 2010), the NRF2 mutant, *skn-1(zu135)* (Tullet et al., 2008), and the mitophagy mutant, *pink-1(ok3538)* (Palikaras et al., 2015) all exhibit significant lifespan extension induced by Δ*lon* (p < 0.001, Figure 7A; Table S6), suggesting their negligible roles in regulating CA-induced longevity. In contrast, the Δ*lon* bacterial mutant was unable to further prolong the lifespan of the *nuo-6(qm200)* or *isp-1(qm150) C. elegans* mutants (Figure 7A; Table S6), neither did the CA supplementation (Figures 7B and 7C; Table S7). Interestingly, both of these *C. elegans* mutants are deficient in the mitochondrial electron transport chain (ETC) (Feng et al., 2001; Ishii et al., 1998; Yang and Hekimi, 2010), suggesting host mitochondria as essential cellular targets of CA.

Mitochondria are highly dynamic organelles and their architecture is shaped by a balance between fusion and fission (Chan,
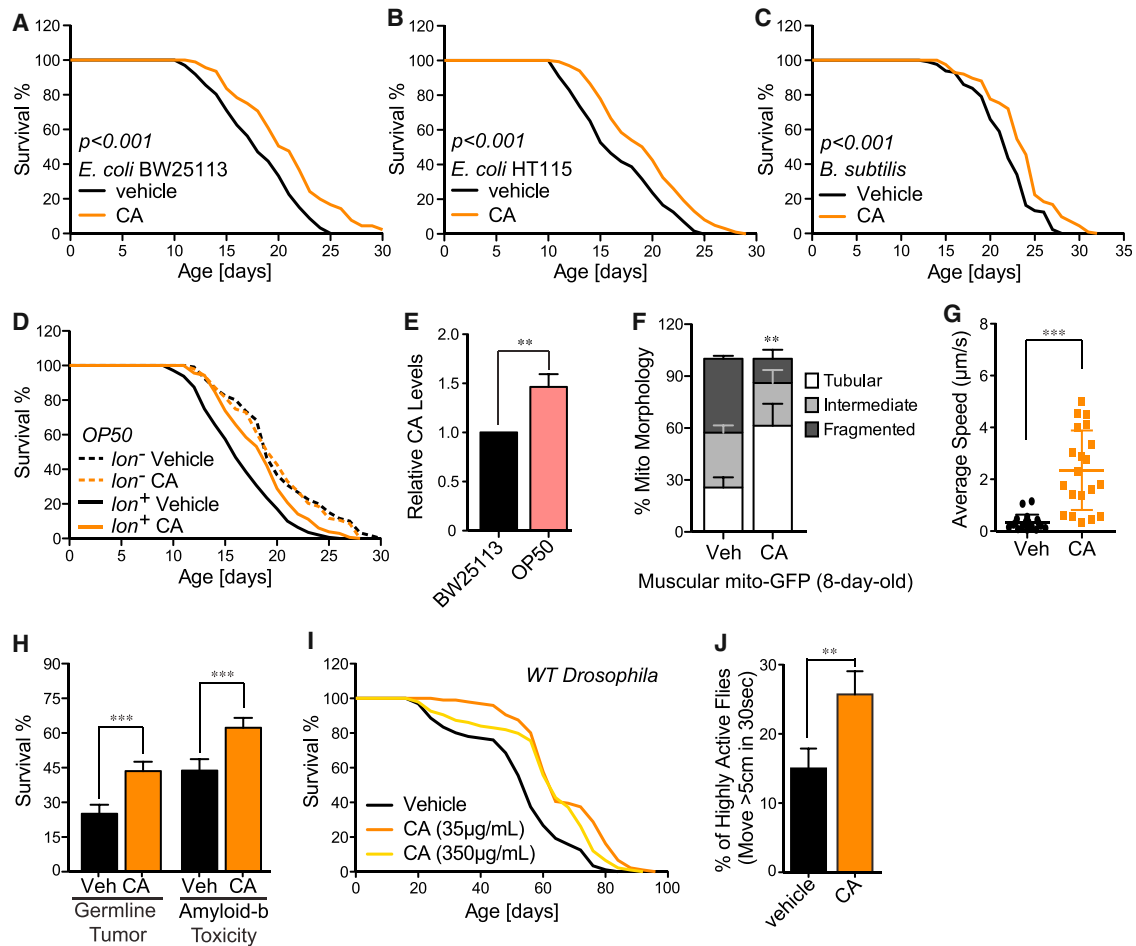
Figure 5. Purified Colanic Acid Promotes Host Longevity across Species

(A–C) CA significantly prolongs the lifespan of wild-type *C. elegans* when supplemented with gram-negative *E. coli* BW25113 (A) and HT115 (B) and with gram-positive *B. subtilis* (C) (p < 0.001, CA versus vehicle control [ddH$_2$O], log rank test).

(D) CA supplementation does not prolong the lifespan of *C. elegans* grown on *lon*-deficient *E. coli* B OP50 (p > 0.5, log rank test) but resumes its effects when *lon* expression is restored in OP50 (p < 0.001, log rank test).

(E) *E. coli* OP50 produces 50% more CA than *E. coli* BW25113 (**p < 0.01, Student's t test).

(F) Muscular cells of 8-day-old *C. elegans* with CA supplementation display significantly increased levels of tubular mitochondrial morphology compared to those on parental control bacteria (**p < 0.01, Student's t test).

(G) CA supplementation increases locomotion velocity of aged *C. elegans,* measured at day 15 of adulthood (***p < 0.0001, non-parametric t test).

(H) CA supplementation increases the survival of the *glp-1(ar202)* tumorous mutants and the transgenic strains expressing human Aβ (***p < 0.001, log rank test).

(I) CA supplementation during adulthood at different concentrations significantly prolongs the lifespan of wild-type *Drosophila OreR* males (p < 0.05, CA versus vehicle control, log rank test).

(J) Fifteen-day-old *Drosophila* adults supplemented with CA have increased mobility, compared to the vehicle controls (**p < 0.01, non-parametric t test).

Error bars represent SEM. See Table S7 for detailed lifespan data including animal numbers, mean and median lifespans, and statistics.

2006). Although the Δ*lon* bacterial mutant did not alter mitochondrial DNA levels, ATP production, or lipid storage (Figures S6A–S6C), we observed that bacterial *lon* deficiency and CA supplementation significantly increase mitochondrial fragmentation in the intestine of *C. elegans* (Figure 7D). Remarkably, mammalian cells treated with CA also display a more fragmented mitochondrial network (Figure 7E), suggesting a highly conserved function of CA in regulating mitochondrial dynamics. Recent studies suggest an association between increased proteasome activity and mitochondrial fragmentation in regulating longevity (Yao et al., 2015). However, we found that CA supplementation has no effect on proteasome activity (Figures S6D–S6F). Next, we examined whether changes of mitochondrial dynamics in the *C. elegans* intestine conferred by CA supplementation are important for its longevity effects. In *C. elegans*, *drp-1* encodes the homolog of yeast Dnm1p and mammalian DRP1 that are required for mitochondrial fission (Breckenridge et al., 2008), and *fzo-1* encodes mitofusin required for mitochondrial fusion (Rolland et al., 2009). We found that intestine-specific knockdown of *drp-1* by RNAi completely abrogates CA-induced lifespan extension (Figure 7F), while intestine-specific knockdown of *fzo-1* does not show such an effect (Figure S6G), suggesting that induction of mitochondrial
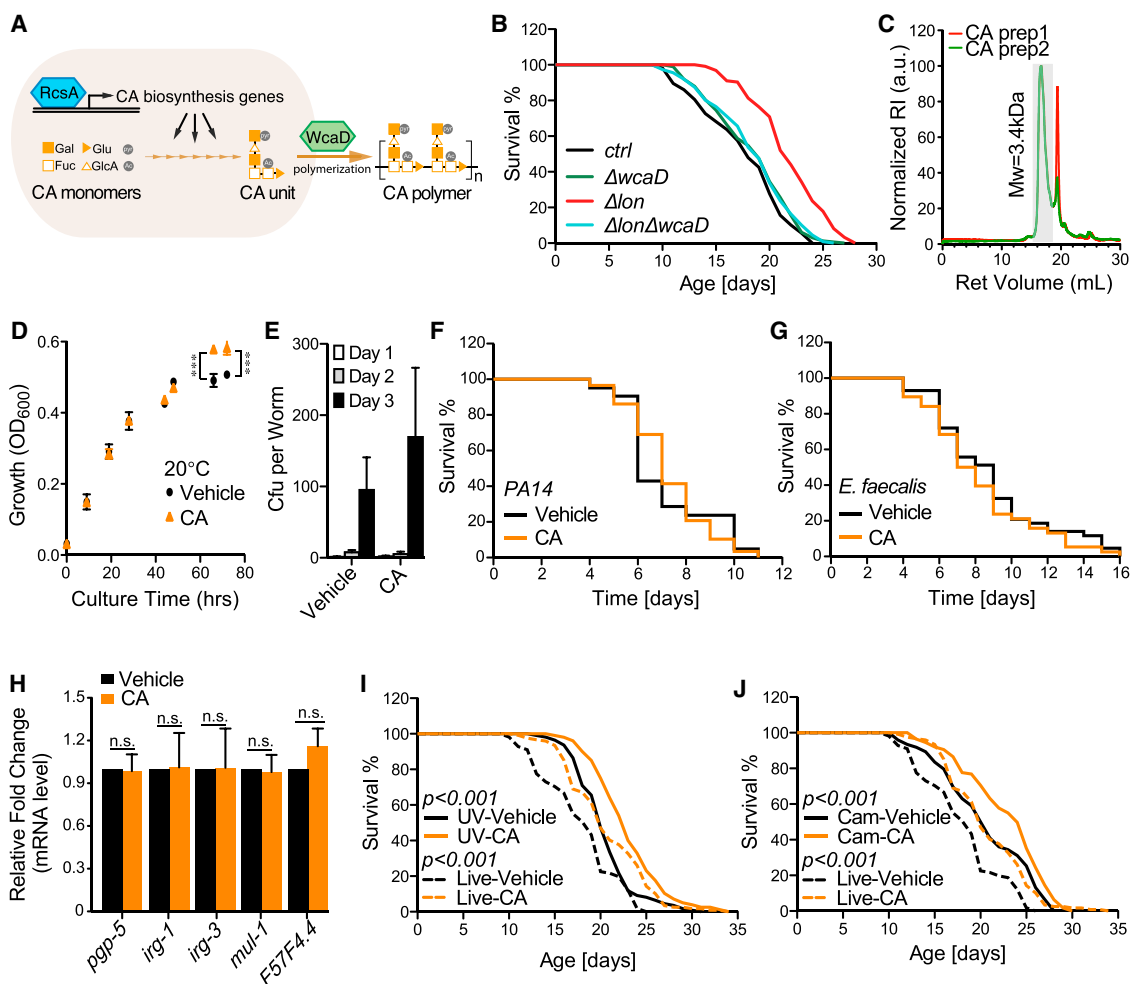
Figure 6. Polymer Forms of CA Act Directly on the Host to Promote Longevity

(A) Schematic depiction of CA polymerization in bacteria. RcsA activates the CA biosynthesis gene cluster. The CA unit contains six monomers, glucose (Glc), galactose (Gal), fucose (Fuc), glucuronic acid (GlcA), pyruvate (Pyr), and acetate (Ac), and is polymerized by WcaD in the periplasm.

(B) Inhibition of CA polymerization by the bacterial ΔwcaD deletion fully suppresses the lifespan extension of *C. elegans* induced by the Δlon bacterial mutant (p > 0.05, ΔwcaDΔlon versus ΔwcaD, log rank test).

(C) Gel permeation chromatography analysis determines the molecular weight of purified CA as ~3.4 kDa. Peaks after 19 mL of retention volume are derived from the solvent.

(D) CA does not reduce bacterial growth. The parental control *E. coli* BW25113 supplemented with water or CA were grown on worm standard plates at 20°C and collected at designated time points to measure OD_{600} (***p < 0.001 CA versus vehicle, Student's t test). Error bars represent SEM.

(E) The colonization of bacteria in the *C. elegans* gut is not affected by CA supplementation (p > 0.5, Student's t test). Error bars represent SEM.

(F and G) CA supplementation does not affect the survival of *C. elegans* infected by *Pseudomonas aeruginosa* PA14 (F) or *Enterococcus faecalis* (G) (p > 0.5, log rank test).

(H) Expressions of five pathogenic response genes are not affected by CA supplementation (non-significant [n.s.] p > 0.5, Student's t test). Error bars represent SD.

(I and J) When supplemented to bacteria killed by UV (I) or inactivated by chloramphenicol (J), CA is still sufficient to prolong lifespan (p < 0.001, CA versus vehicle control, log rank test). Experiments were conducted in parallel with same live-bacteria controls (vehicle and CA-treated).

See Figure S5 for lifespan data on CA monomers/unit, other polysaccharides, and CA with endocytosis mutants, and Tables S6 and S7 for lifespan data including animal numbers, mean and median lifespans, and statistics.

fission, but not fusion, in the host gut is responsible for CA-induced longevity. Furthermore, mild induction of intestinal mitochondrial fragmentation by tissue-specific overexpression of *drp-1* sufficiently increased *C. elegans* lifespan (Figure 7G).

In addition to its effects on mitochondrial dynamics, we found that CA also modulates mitochondrial unfolded protein re-

sponses (UPRmt) under stress conditions. UPRmt has previously been linked to mitochondrial homeostasis and longevity, which can be denoted by induced expression of *C. elegans* mitochondrial chaperone HSP-6 (Pellegrino et al., 2013). When protein folding in mitochondria is comprised by inactivation of the mitochondrial intermediate peptidase gene, *mip-1(Y67H2A.7)*, CA
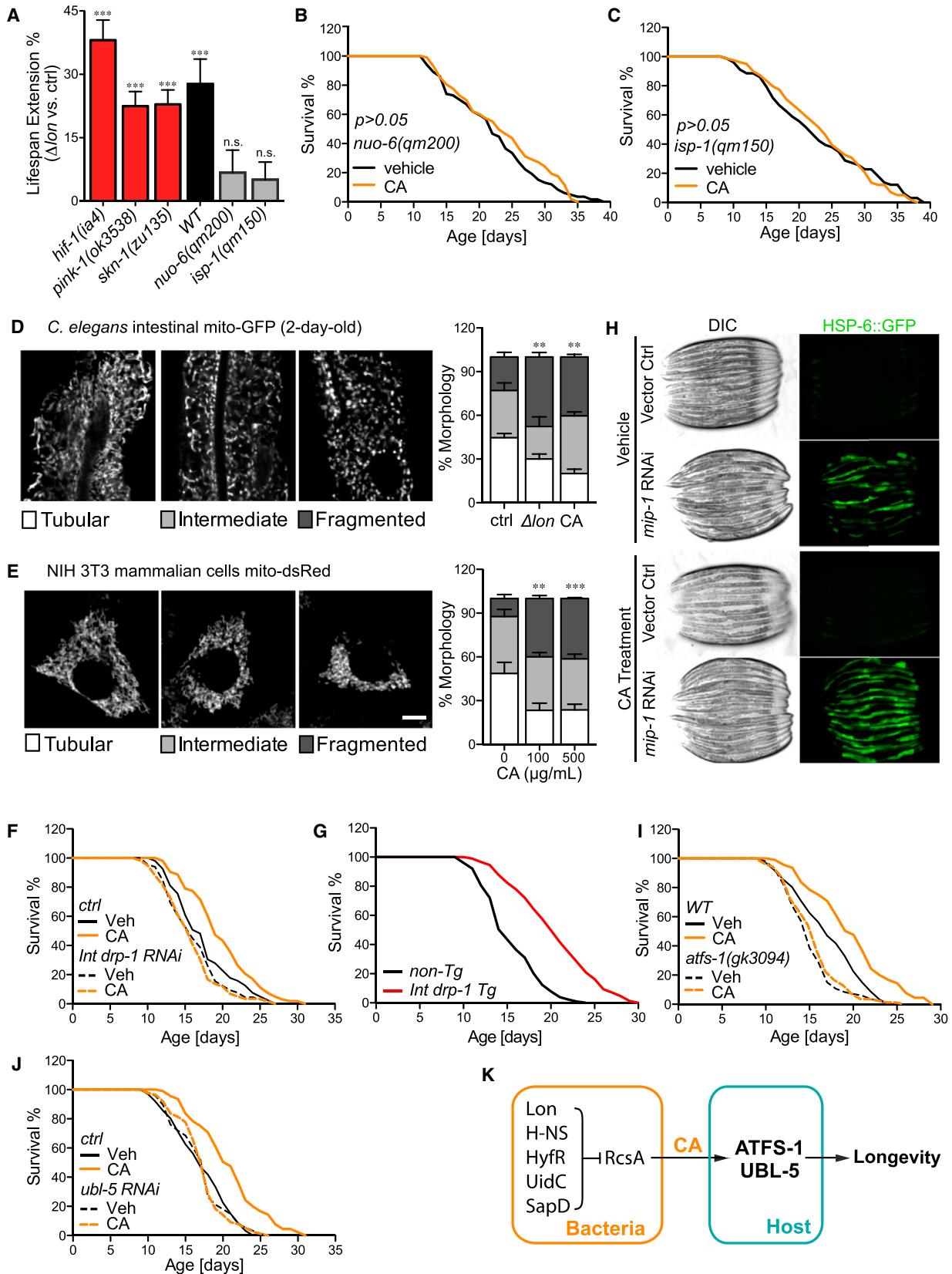
(legend on next page)

supplementation significantly exaggerated the induction of HSP-6 (Figure 7H), suggesting enhanced UPR^{mt} by CA under mitochondrial stress conditions. However, in absence of mitochondrial stress, we found no noticeable induction of UPR^{mt} by CA (Figure 7H), suggesting that CA does not directly disrupt mitochondrial protein-folding homeostasis.

ATFS-1 is a key transcription factor that regulates UPR^{mt} and forms a complex with UBL-5 and DVE-1 to induce transcription of mitochondrial chaperones (Andreux et al., 2013). We found that the loss-of-function atfs-1(gk3094) mutant completely suppresses the lifespan-extending effect of CA (Figure 7I; Table S7). Similarly, RNAi knockdown of ubl-5 also fully abrogated CA-induced longevity (Figure 7J; Table S7). These results reveal that the effect of bacterial CA on host longevity requires the UPR^{mt} signaling pathway (Figure 7K).

DISCUSSION

Our studies reveal the significance of microbial genetic variations in modulating host longevity. The microbiota not only comprise diverse microbial species, but they also exhibit profound genetic heterogeneity within each species. Genetic drift frequently occurs in microbes, and microbial gene expression is dynamically influenced by environmental stimuli in the host gut. In a model organism C. elegans, we systematically identified bacterial genes whose deletion leads to lifespan extension and revealed the potential of a dozen of these bacterial mutants in attenuating lethality due to age-associated progression of germline tumor and accumulation of pathological Aβ. Interestingly, these identified bacterial genes are highly heterogeneous in their functions spanning many aspects of bacterial morphology and physiology (Figure 1), which implies a number of discrete mechanisms that await individual characterization.

Using genetic and biochemical analyses, we discovered overproducing CA polysaccharide as a longevity-promoting mechanism. In parallel, functional gene ontology analysis on our screening hits reveals the enrichment of genes involved in chorismate metabolism (Figure S7). This molecule is a biochemical precursor for many aromatic metabolites (Bentley, 1990). Synthetic deficiencies in two of the chorismate derivatives, ubiquinone and folate, underlie the prolonged host lifespan by the E. coli mutants previously identified (Saiki et al., 2008; Virk et al., 2012). A life-prolonging drug metformin exerts its beneficial effects by interfering with bacterial methionine biosynthesis, which is also coupled with chorismate metabolism (Cabreiro et al., 2013). Thus, manipulating chorismate biosynthesis in intestinal microbes may be a promising strategy to promote host longevity. Our results also demonstrate that microbial CA overproduction and chorismate deficiency function in parallel pathways to promote host longevity and exert additive effects when combined.

The majority of our identified bacterial genes sustain their abilities in influencing host longevity when deleted in distinct bacterial backgrounds and do not require presence during C. elegans development to exert their longevity-promoting effects. Therefore, our studies mark their probable merits in taking effects across diverse gut inhabitants and for late-life intervention. In addition, these bacterial mutants interact with one or more longevity regulatory mechanisms in the host, including insulin/IGF-1 signaling, TOR signaling, caloric restriction, and mitochondrial hormesis, suggesting that altering bacterial genetic composition could be an effective way to activate major host longevity signaling and promote healthy aging. On the other hand, mechanistic dissection of each longevity-promoting bacterial mutant may highlight specific molecules that can directly act on the host, such as CA. Effective in several host-microbe environments and pursuant further tests in mammalian systems, CA may provide an exciting approach for improving human health and longevity.

Mitochondria, which have been linked to aging processes, are not only the metabolic center of the cell, but also key signaling organelles (Riera and Dillin, 2015). Mitochondrial hormesis in the nervous system has been previously shown to generate systemic signals and exert beneficial effects cell non-autonomously

---

Figure 7. CA Acts on Host Mitochondria to Promote Longevity

(A) The Δlon bacterial mutant extends the lifespan of C. elegans hif-1(ia4), skn-1(zu135), and pink-1(ok3538) mutants but is not able to do so in the mutants of C. elegans ETC components, nuo-6(qm200) or isp-1(qm15) (***p < 0.001, n.s. p > 0.05, Δlon versus parental control, log rank test). Error bars represent SEM.

(B and C) CA supplementation cannot further increase the lifespan extension conferred by the mitochondrial ETC mutations, nuo-6(qm200) (B) and isp-1(qm150) (C) (p > 0.05, CA versus vehicle control, log rank test).

(D) Both the Δlon mutant and CA supplementation increase mitochondrial fragmentation in C. elegans intestinal cells (**p < 0.01, Student's t test). The transgenic strain expressing mito-GFP in the intestine (raxIs[ges-1p::mitoGFP]) was analyzed at day 2 adulthood. As shown in representative images, mitochondrial morphologies are categorized as either tubular, intermediate, or fragmented. Scale bar, 10 μm. Error bars represent SEM.

(E) CA increases mitochondrial fragmentation in mammalian cells (**p < 0.01, ***p < 0.001, Student's t test). Mitochondrial morphologies were analyzed in the NIH/3T3 mammalian cells stably expressing dsRed2-mito, categorized as either tubular, intermediate, or fragmented. Representative images are shown. Scale bar, 10 μm. Error bars represent SEM.

(F) Intestinal-specific knockdown of drp-1 by RNAi fully suppresses the lifespan extension conferred by CA (p > 0.05, CA versus vehicle control [drp-1 RNAi], log rank test).

(G) Intestinal-specific overexpression of drp-1 is sufficient to increase the lifespan of C. elegans (p < 0.001 compared to non-transgenic siblings by log rank test).

(H) The level of mitochondrial chaperone HSP-6::GFP was used to measure UPR^{mt}. Inactivation of mitochondrial intermediate peptidase, mip-1(Y67H2A.7) by RNAi induces the HSP-6::GFP level, which is further elevated by CA supplementation.

(I) In the loss-of-function mutant of atfs-1(gk3094), the lifespan extension conferred by CA supplementation is fully suppressed (p > 0.05, CA versus vehicle control [atfs-1], log rank test).

(J) RNAi knockdown of ubl-5 completely abrogates the lifespan-extending effect of CA (p > 0.05, CA versus vehicle control [ubl-5 RNAi], log rank test).

(K) A diagram of CA-mediated bacteria-host communication in regulating host longevity.

See Figure S6 for additional information of CA effects on mitochondria, lipid storage, and proteasome and Tables S6 and S7 for lifespan data including animal numbers, mean and median lifespans, and statistics.

in distal tissues (Durieux et al., 2011). Our studies show that CA enhances UPR^{mt} and triggers mitochondrial fragmentation in the intestine and prolongs host lifespan via interacting with mitochondrial ETC complexes. These different impacts of CA on mitochondria can be integrated by the action of ATFS-1, as supported by previous studies showing that reduction in mitochondrial ETC components causes a strong activation of UPR^{mt} (Durieux et al., 2011; Houtkooper et al., 2013), the activation of ATFS-1 by UPR^{mt} suppresses the expression of ETC genes in both the nuclear and mitochondrial genomes (Nargund et al., 2015), and ATFS-1 induces the expression of the mitochondrial fission protein DRP-1 (Nargund et al., 2015). Our studies demonstrate ATFS-1 as a key mediator of the CA longevity effect. Therefore, the intestine is another key tissue for mitochondrial signals to regulate the rate of aging systemically, and CA can trigger this mitochondrial signaling.

The discovery of CA's modes of action reveals an intriguing crosstalk between mitochondria and symbiotic bacteria in animal hosts. Mitochondria evolved from and share many metabolic pathways with bacteria (Andersson et al., 1998). Conceptually, the microbiota may influence the host similarly as mitochondria do, by chemically communicating with their ancient intra-cellular relatives. CA is a case in point, serving as a messenger for this type of dialog. Synthesized in bulk upon environmental stress (Chen et al., 2004), bacterial CA induces mitochondrial fragmentation and UPR^{mt}, which consequently generates systemic signals to improve host fitness. In this sense, animals can perceive stress-associated information from their gut microbiota and get physiologically ready for upcoming unfavorable conditions, likely a result of coevolution. Empirically, future investigations on bacteria-mitochondria communications might open up new avenues for treating human mitochondrial diseases and aging.

STAR★METHODS

Detailed methods are provided in the online version of this paper and include the following:

- KEY RESOURCES TABLE
- CONTACT FOR REAGENT AND RESOURCE SHARING
- EXPERIMENTAL MODEL AND SUBJECT DETAILS
  - ○ Animals
  - ○ Microbe strains
  - ○ Cell lines
- METHOD DETAILS
  - ○ Genomic screen
  - ○ Bacterial growth and colonization analyses
  - ○ P1 phage transduction
  - ○ Restoration of lon functionality
  - ○ Quantification of CA
  - ○ Purification and administration of CA
  - ○ Lifespan and paralysis assays
  - ○ Developmental time and brood size analyses
  - ○ Pharyngeal pumping, defecation cycle, and locomotion activity measurement
  - ○ Gel permeation chromatography analysis
  - ○ Quantitative PCR analyses
  - ○ ATP quantification
  - ○ Quantification of peptidase activities of the proteasome
  - ○ Mitochondrial morphology assays and stimulated Raman scattering microscopy
- QUANTIFICATION AND STATISTICAL ANALYSIS

REFERENCES

Andersson, S.G., Zomorodipour, A., Andersson, J.O., Sicheritz-Pontén, T., Alsmark, U.C., Podowski, R.M., Näslund, A.K., Eriksson, A.S., Winkler, H.H., and Kurland, C.G. (1998). The genome sequence of Rickettsia prowazekii and the origin of mitochondria. Nature 396, 133–140.

Andreux, P.A., Houtkooper, R.H., and Auwerx, J. (2013). Pharmacological approaches to restore mitochondrial function. Nat. Rev. Drug Discov. 12, 465–483.

Baba, T., Ara, T., Hasegawa, M., Takai, Y., Okumura, Y., Baba, M., Datsenko, K.A., Tomita, M., Wanner, B.L., and Mori, H. (2006). Construction of Escherichia coli K-12 in-frame, single-gene knockout mutants: the Keio collection. Mol. Syst. Biol. 2, 2006.0008.

Bentley, R. (1990). The shikimate pathway–a metabolic tree with many branches. Crit. Rev. Biochem. Mol. Biol. 25, 307–384.

Breckenridge, D.G., Kang, B.H., Kokel, D., Mitani, S., Staehelin, L.A., and Xue, D. (2008). Caenorhabditis elegans drp-1 and fis-2 regulate distinct cell-death execution pathways downstream of ced-3 and independent of ced-9. Mol. Cell 31, 586–597.

Cabreiro, F., Au, C., Leung, K.Y., Vergara-Irigaray, N., Cochemé, H.M., Noori, T., Weinkove, D., Schuster, E., Greene, N.D., and Gems, D. (2013). Metformin retards aging in C. elegans by altering microbial folate and methionine metabolism. Cell 153, 228–239.

Chan, D.C. (2006). Mitochondria: dynamic organelles in disease, aging, and development. Cell 125, 1241–1252.

Chen, J., Lee, S.M., and Mao, Y. (2004). Protective effect of exopolysaccharide colanic acid of Escherichia coli O157:H7 to osmotic and oxidative stress. Int. J. Food Microbiol. 93, 281–286.

Cho, I., and Blaser, M.J. (2012). The human microbiome: at the interface of health and disease. Nat. Rev. Genet. *13*, 260–270.

Claesson, M.J., Jeffery, I.B., Conde, S., Power, S.E., O'Connor, E.M., Cusack, S., Harris, H.M., Coakley, M., Lakshminarayanan, B., O'Sullivan, O., et al. (2012). Gut microbiota composition correlates with diet and health in the elderly. Nature *488*, 178–184.

Clark, L.C., and Hodgkin, J. (2014). Commensals, probiotics and pathogens in the Caenorhabditis elegans model. Cell. Microbiol. *16*, 27–38.

Dische, Z., and Shettles, L.B. (1948). A specific color reaction of methylpentoses and a spectrophotometric micromethod for their determination. J. Biol. Chem. *175*, 595–603.

Durieux, J., Wolff, S., and Dillin, A. (2011). The cell-non-autonomous nature of electron transport chain-mediated longevity. Cell *144*, 79–91.

Feng, J., Bussière, F., and Hekimi, S. (2001). Mitochondrial electron transport is a key determinant of life span in Caenorhabditis elegans. Dev. Cell *1*, 633–644.

Fontana, L., Partridge, L., and Longo, V.D. (2010). Extending healthy life span–from yeast to humans. Science *328*, 321–326.

Garigan, D., Hsu, A.L., Fraser, A.G., Kamath, R.S., Ahringer, J., and Kenyon, C. (2002). Genetic analysis of tissue aging in Caenorhabditis elegans: a role for heat-shock factor and bacterial proliferation. Genetics *161*, 1101–1112.

Gottesman, S., Trisler, P., and Torres-Cabassa, A. (1985). Regulation of capsular polysaccharide synthesis in Escherichia coli K-12: characterization of three regulatory genes. J. Bacteriol. *162*, 1111–1119.

Grant, W.D., Sutherland, I.W., and Wilkinson, J.F. (1969). Exopolysaccharide colanic acid and its occurrence in the Enterobacteriaceae. J. Bacteriol. *100*, 1187–1193.

Grant, B., Zhang, Y., Paupard, M.C., Lin, S.X., Hall, D.H., and Hirsh, D. (2001). Evidence that RME-1, a conserved C. elegans EH-domain protein, functions in endocytic recycling. Nat. Cell Biol. *3*, 573–579.

Gusarov, I., Gautier, L., Smolentseva, O., Shamovsky, I., Eremina, S., Mironov, A., and Nudler, E. (2013). Bacterial nitric oxide extends the lifespan of C. elegans. Cell *152*, 818–830.

Harrison, D.E., Strong, R., Sharp, Z.D., Nelson, J.F., Astle, C.M., Flurkey, K., Nadon, N.L., Wilkinson, J.E., Frenkel, K., Carter, C.S., et al. (2009). Rapamycin fed late in life extends lifespan in genetically heterogeneous mice. Nature *460*, 392–395.

Harrison, D.E., Strong, R., Allison, D.B., Ames, B.N., Astle, C.M., Atamna, H., Fernandez, E., Flurkey, K., Javors, M.A., Nadon, N.L., et al. (2014). Acarbose, 17-α-estradiol, and nordihydroguaiaretic acid extend mouse lifespan preferentially in males. Aging Cell *13*, 273–282.

Heintz, C., and Mair, W. (2014). You are what you host: microbiome modulation of the aging process. Cell *156*, 408–411.

Houtkooper, R.H., Mouchiroud, L., Ryu, D., Moullan, N., Katsyuba, E., Knott, G., Williams, R.W., and Auwerx, J. (2013). Mitonuclear protein imbalance as a conserved longevity mechanism. Nature *497*, 451–457.

Howitz, K.T., Bitterman, K.J., Cohen, H.Y., Lamming, D.W., Lavu, S., Wood, J.G., Zipkin, R.E., Chung, P., Kisielewski, A., Zhang, L.L., et al. (2003). Small molecule activators of sirtuins extend Saccharomyces cerevisiae lifespan. Nature *425*, 191–196.

Ishii, N., Fujii, M., Hartman, P.S., Tsuda, M., Yasuda, K., Senoo-Matsuda, N., Yanase, S., Ayusawa, D., and Suzuki, K. (1998). A mutation in succinate dehydrogenase cytochrome b causes oxidative stress and ageing in nematodes. Nature *394*, 694–697.

Kenyon, C.J. (2010). The genetics of ageing. Nature *464*, 504–512.

Lakowski, B., and Hekimi, S. (1998). The genetics of caloric restriction in Caenorhabditis elegans. Proc. Natl. Acad. Sci. USA *95*, 13091–13096.

Larsen, P.L., and Clarke, C.F. (2002). Extension of life-span in Caenorhabditis elegans by a diet lacking coenzyme Q. Science *295*, 120–123.

Lee, W.J., and Hase, K. (2014). Gut microbiota-generated metabolites in animal health and disease. Nat. Chem. Biol. *10*, 416–424.

Leiser, S.F., and Kaeberlein, M. (2010). The hypoxia-inducible factor HIF-1 functions as both a positive and negative modulator of aging. Biol. Chem. *391*, 1131–1137.

Lin, K., Dorman, J.B., Rodan, A., and Kenyon, C. (1997). daf-16: An HNF-3/forkhead family member that can function to double the life-span of Caenorhabditis elegans. Science *278*, 1319–1322.

Link, C.D. (1995). Expression of human beta-amyloid peptide in transgenic Caenorhabditis elegans. Proc. Natl. Acad. Sci. USA *92*, 9368–9372.

Liu, H., Wang, X., Wang, H.D., Wu, J., Ren, J., Meng, L., Wu, Q., Dong, H., Wu, J., Kao, T.Y., et al. (2012). Escherichia coli noncoding RNAs can affect gene expression and physiology of Caenorhabditis elegans. Nat. Commun. *3*, 1073.

Mizunuma, M., Neumann-Haefelin, E., Moroz, N., Li, Y., and Blackwell, T.K. (2014). mTORC2-SGK-1 acts in two environmentally responsive pathways with opposing effects on longevity. Aging Cell *13*, 869–878.

Nargund, A.M., Fiorese, C.J., Pellegrino, M.W., Deng, P., and Haynes, C.M. (2015). Mitochondrial and nuclear accumulation of the transcription factor ATFS-1 promotes OXPHOS recovery during the UPR(mt). Mol. Cell *58*, 123–133.

Niccoli, T., and Partridge, L. (2012). Ageing as a risk factor for disease. Curr. Biol. *22*, R741–R752.

Ogg, S., Paradis, S., Gottlieb, S., Patterson, G.I., Lee, L., Tissenbaum, H.A., and Ruvkun, G. (1997). The Fork head transcription factor DAF-16 transduces insulin-like metabolic and longevity signals in C. elegans. Nature *389*, 994–999.

Oh, S.W., Mukhopadhyay, A., Svrzikapa, N., Jiang, F., Davis, R.J., and Tissenbaum, H.A. (2005). JNK regulates lifespan in Caenorhabditis elegans by modulating nuclear translocation of forkhead transcription factor/DAF-16. Proc. Natl. Acad. Sci. USA *102*, 4494–4499.

Palikaras, K., Lionaki, E., and Tavernarakis, N. (2015). Coupling mitogenesis and mitophagy for longevity. Autophagy *11*, 1428–1430.

Pan, K.Z., Palter, J.E., Rogers, A.N., Olsen, A., Chen, D., Lithgow, G.J., and Kapahi, P. (2007). Inhibition of mRNA translation extends lifespan in Caenorhabditis elegans. Aging Cell *6*, 111–119.

Pellegrino, M.W., Nargund, A.M., and Haynes, C.M. (2013). Signaling the mitochondrial unfolded protein response. Biochim. Biophys. Acta *1833*, 410–416.

Pepper, A.S., Lo, T.W., Killian, D.J., Hall, D.H., and Hubbard, E.J. (2003). The establishment of Caenorhabditis elegans germline pattern is controlled by overlapping proximal and distal somatic gonad signals. Dev. Biol. *259*, 336–350.

Portal-Celhay, C., Bradley, E.R., and Blaser, M.J. (2012). Control of intestinal bacterial proliferation in regulation of lifespan in Caenorhabditis elegans. BMC Microbiol. *12*, 49.

Ramachandran, P.V., Mutlu, A.S., and Wang, M.C. (2015). Label-free biomedical imaging of lipids by stimulated Raman scattering microscopy. Curr. Protoc. Mol. Biol. *109*, 30.3.1-17.

Regmi, S.G., Rolland, S.G., and Conradt, B. (2014). Age-dependent changes in mitochondrial morphology and volume are not predictors of lifespan. Aging (Albany NY) *6*, 118–130.

Riera, C.E., and Dillin, A. (2015). Tipping the metabolic scales towards increased longevity in mammals. Nat. Cell Biol. *17*, 196–203.

Robida-Stubbs, S., Glover-Cutter, K., Lamming, D.W., Mizunuma, M., Narasimhan, S.D., Neumann-Haefelin, E., Sabatini, D.M., and Blackwell, T.K. (2012). TOR signaling and rapamycin influence longevity by regulating SKN-1/Nrf and DAF-16/FoxO. Cell Metab. *15*, 713–724.

Rolland, S.G., Lu, Y., David, C.N., and Conradt, B. (2009). The BCL-2-like protein CED-9 of C. elegans promotes FZO-1/Mfn1,2- and EAT-3/Opa1-dependent mitochondrial fusion. J. Cell Biol. *186*, 525–540.

Saiki, R., Lunceford, A.L., Bixler, T., Dang, P., Lee, W., Furukawa, S., Larsen, P.L., and Clarke, C.F. (2008). Altered bacterial metabolism, not coenzyme Q content, is responsible for the lifespan extension in Caenorhabditis elegans fed an Escherichia coli diet lacking coenzyme Q. Aging Cell *7*, 291–304.

Sledjeski, D., and Gottesman, S. (1995). A small RNA acts as an antisilencer of the H-NS-silenced rcsA gene of Escherichia coli. Proc. Natl. Acad. Sci. USA *92*, 2003–2007.

Soukas, A.A., Kane, E.A., Carr, C.E., Melo, J.A., and Ruvkun, G. (2009). Rictor/TORC2 regulates fat metabolism, feeding, growth, and life span in Caenorhabditis elegans. Genes Dev. *23*, 496–511.

Stanfel, M.N., Shamieh, L.S., Kaeberlein, M., and Kennedy, B.K. (2009). The TOR pathway comes of age. Biochim Biophys Acta. *1790*, 1067–1074.

Stevenson, G., Andrianopoulos, K., Hobbs, M., and Reeves, P.R. (1996). Organization of the Escherichia coli K-12 gene cluster responsible for production of the extracellular polysaccharide colanic acid. J. Bacteriol. *178*, 4885–4893.

Sulston, J.E., and Brenner, S. (1974). The DNA of Caenorhabditis elegans. Genetics *77*, 95–104.

Sutherland, I.W. (1969). Structural studies on colanic acid, the common exopolysaccharide found in the enterobacteriaceae, by partial acid hydrolysis. Oligosaccharides from colanic acid. Biochem. J. *115*, 935–945.

Torres-Cabassa, A.S., and Gottesman, S. (1987). Capsule synthesis in Escherichia coli K-12 is regulated by proteolysis. J. Bacteriol. *169*, 981–989.

Tullet, J.M., Hertweck, M., An, J.H., Baker, J., Hwang, J.Y., Liu, S., Oliveira, R.P., Baumeister, R., and Blackwell, T.K. (2008). Direct inhibition of the longevity-promoting factor SKN-1 by insulin-like signaling in C. elegans. Cell *132*, 1025–1038.

Virk, B., Correia, G., Dixon, D.P., Feyst, I., Jia, J., Oberleitner, N., Briggs, Z., Hodge, E., Edwards, R., Ward, J., et al. (2012). Excessive folate synthesis limits lifespan in the C. elegans: E. coli aging model. BMC Biol. *10*, 67.

Wang, M.C., Bohmann, D., and Jasper, H. (2005). JNK extends life span and limits growth by antagonizing cellular and organism-wide responses to insulin signaling. Cell *121*, 115–125.

Wang, M.C., Min, W., Freudiger, C.W., Ruvkun, G., and Xie, X.S. (2011). RNAi screening for fat regulatory genes with SRS microscopy. Nat. Methods *8*, 135–138.

Wang, M.C., Oakley, H.D., Carr, C.E., Sowa, J.N., and Ruvkun, G. (2014). Gene pathways that delay Caenorhabditis elegans reproductive senescence. PLoS Genet. *10*, e1004752.

Williams, B.D., Schrank, B., Huynh, C., Shownkeen, R., and Waterston, R.H. (1992). A genetic mapping system in Caenorhabditis elegans based on polymorphic sequence-tagged sites. Genetics *131*, 609–624.

Yang, W., and Hekimi, S. (2010). Two modes of mitochondrial dysfunction lead independently to lifespan extension in Caenorhabditis elegans. Aging Cell *9*, 433–447.

Yao, Y., Tsuchiyama, S., Yang, C., Bulteau, A.L., He, C., Robison, B., Tsuchiya, M., Miller, D., Briones, V., Tar, K., et al. (2015). Proteasomes, Sir2, and Hxk2 form an interconnected aging network that impinges on the AMPK/Snf1-regulated transcriptional repressor Mig1. PLoS Genet. *1*, e1004968.

Yatsunenko, T., Rey, F.E., Manary, M.J., Trehan, I., Dominguez-Bello, M.G., Contreras, M., Magris, M., Hidalgo, G., Baldassano, R.N., Anokhin, A.P., et al. (2012). Human gut microbiome viewed across age and geography. Nature *486*, 222–227.

STAR★METHODS

KEY RESOURCES TABLE

REAGENT or RESOURCE	SOURCE	IDENTIFIER
Bacterial and Virus Strains		
E. coli: Strain OP50	Caenorhabditis Genetics Center	WormBase: OP50
E. coli: Strain HT115	Caenorhabditis Genetics Center	WormBase: HT115
E. coli: Strain MG1655	Laboratory of J. J. Wang	J. J. Wang
E. coli: Ahringer collection	Laboratory of M. Wang	M. Wang
E. coli: Keio collection	Laboratory of C. Herman	C. Herman
B. subtilis	Laboratory of J. J. Wang	J. J. Wang
P. aeruginosa: Strain PA14	Laboratory of D. A. Garsin	D. A. Garsin
E. faecalis	Laboratory of D. A. Garsin	D. A. Garsin
Enterobacteria phage P1	Laboratory of C. Herman	C. Herman
Chemicals, Peptides, and Recombinant Proteins		
hyaluronic acid sodium salt	Sigma-Aldrich	CAS Number: 9067-32-7
alginic acid	Sigma-Aldrich	CAS Number: 9005-32-7
Fluorogenic peptide: Suc-LLVY-AMC	Bachem	I-1395.0025
Fluorogenic peptide: Ac-RLR-AMC	Bachem	I-1955.0001
Fluorogenic peptide: Ac-nLPnLD-AMC	Bachem	I-1850.0005
Critical Commercial Assays		
ATP Determination Kit	Invitrogen	A22066
Pierce BCA Protein Assay Kit	Thermo Scientific	23225
Power SYBR Green Cells-to-Ct Kit	ThermoFisher Scientific	4402953
KAPA SYBR FAST qPCR Master Mix (2X) Kit	Kapa Biosystems	07959427001
Experimental Models: Cell Lines		
M. musculus: Cell line NIH/3T3 expressing dsRed2-Mito	Michael A Frohman	PMID: 17028579
Experimental Models: Organisms/Strains		
C. elegans: Strain N2: wild isolate	Caenorhabditis Genetics Center	WormBase: N2
C. elegans: Strain CB4121: *sqt-3(e2117)* V	Caenorhabditis Genetics Center	WormBase: CB4121
C. elegans: Strain GC833: *glp-1(ar202)* III	Caenorhabditis Genetics Center	WormBase: GC833
C. elegans: Strain: *daf-16(mgDf47)* I	Laboratory of G. Ruvkun	N/A
C. elegans: Strain RB1206: *rsks-1(ok1255)* III	Caenorhabditis Genetics Center	WormBase: RB1206
C. elegans: Strain VC222: *raga-1(ok386)* II	Caenorhabditis Genetics Center	WormBase: VC222
C. elegans: Strain KQ1366: *rict-1(ft7)* II	Caenorhabditis Genetics Center	WormBase: KQ1366
C. elegans: Strain DA465: *eat-2(ad465)* II	Caenorhabditis Genetics Center	WormBase: DA465
C. elegans: Strain DA1116: *eat-2(ad1116)* II	Caenorhabditis Genetics Center	WormBase: DA1116
C. elegans: Strain MQ887: *isp-1(qm15)* IV	Caenorhabditis Genetics Center	WormBase: MQ887
C. elegans: Strain MQ1333: *nuo-6(qm200)* I	Caenorhabditis Genetics Center	WormBase: MQ1333
C. elegans: Strain KU25: *pmk-1(km25)* IV	Caenorhabditis Genetics Center	WormBase: KU25
C. elegans: Strain VC3056: *zip-2(ok3730)* III	Caenorhabditis Genetics Center	WormBase: VC3056
C. elegans: Strain RB2547: *pink-1(ok3538)* II	Caenorhabditis Genetics Center	WormBase: RB2547
C. elegans: Strain ZG31: *hif-1(ia4)* V	Caenorhabditis Genetics Center	WormBase: ZG31
C. elegans: Strain VC3201: *atfs-1(gk3094)* V	Caenorhabditis Genetics Center	WormBase: VC3201
C. elegans: Strain VC308: *rab-7(ok511)/mIn1* [mIs14 *dpy-10(e128)*] II.	Caenorhabditis Genetics Center	WormBase: VC308

(Continued on next page)

Continued

REAGENT or RESOURCE	SOURCE	IDENTIFIER
C. elegans: Strain LG340: skn-1(zu135) IV/nT1 [qIs51] (IV;V); geEx1[gpa-4p::skn-1b::GFP + rol-6(su1006)].	Caenorhabditis Genetics Center	WormBase: LG340
C. elegans: Strain SJ4100: zcIs13[hsp-6p::GFP]	Caenorhabditis Genetics Center	WormBase: SJ4100
C. elegans: Strain JM45: rde-1(ne219); Is [ges-1p::rde-1::unc54 3′UTR; myo2p::RFP3]	Laboratory of J. Mello	N/A
C. elegans: Strain: Ex[ges-1p::drp-1::sl2GFP; myo-2p::mCherry]	This paper	N/A
C. elegans: Strain: raxIs[ges-1p::mitoGFP]	This paper	N/A
C. elegans: Strain: raxIs[myo-3p::mitoGFP]	This paper	N/A
C. briggsae: Strain DH1300: wild isolate	Caenorhabditis Genetics Center	WormBase: DH1300
P. redivivus: Strain PS2298: wild isolate	Caenorhabditis Genetics Center	WormBase: PS2298
D. melanogaster: Strain OreR	Laboratory of H. Dierick	H. Dierick
Oligonucleotides		
See Table S8 for primer sequences		

CONTACT FOR REAGENT AND RESOURCE SHARING

Further information and requests for resources and reagents should be directed to and will be fulfilled by the Lead Contact, Meng C. Wang (wmeng@bcm.edu).

EXPERIMENTAL MODEL AND SUBJECT DETAILS

Animals

The nematodes C. elegans, C. briggsae, and P. redivivus were mostly obtained from the Caenorhabditis Genome Center. Some nematode strains were gifts from other labs or generated in the lab. The nematodes were maintained and experimentally examined at 20°C on standard nematode growth medium (NGM) agar plates seeded with pre-cultured bacterial strains unless otherwise noted. Hermaphrodites of C. elegans and C. briggsae were age-synchronized by isolating eggs as previously described (Sulston and Brenner, 1974). Female P. redivivus were synchronized by collecting newly produced larvae within a time window of 2 hr. The Drosophila melanogaster OreR strain was reared and assayed at 25°C with a 12h:12h light-dark cycle. During the experiments, the flies were allowed to develop and mate for two days after eclosion, and then were sexually segregated. In all cases, individual animals were assigned randomly into different experimental groups.

Microbe strains

For primary screens, E. coli Keio mutants were grown overnight at 37°C in Luria-Broth (LB) medium added with 10 μg/mL kanamycin. 150 μL of the bacteria culture was seeded to each well of 12-well NGM plates. For longitudinal assays, E. coli were cultivated in LB medium at 37°C for 9 hr. Centrifuged bacteria pellets were washed using M9 buffer for three times, and re-suspended in M9 buffer to a concentration whose 20-fold dilution exhibits an OD_{600} between 0.15 and 0.16. A microscopic counting chamber was used to confirm the variations of bacterial cell numbers less than 10%. 350 μL of the bacteria suspension was seeded on each 6cm NGM plate.

For lifespan assays with CA supplementation, E. coli, B. subtilis, and P. aeruginosa were cultured in LB medium overnight while E. faecalis was grown in Brain-heart infusion medium (BHI) for 5 hr. The bacteria culture was then mixed with half volume of either CA solution or ddH_2O as control before seeded onto plates. NGM plates were used for E. coli and B. subtilis, slow-killing (SK) plates were used for P. aeruginosa, and BHI plates with gentamicin were used for E. faecalis. The NGM plates were incubated at 20°C for 2 days while both the SK and BHI plates were incubated at 37°C overnight.

For RNAi knockdown of selected worm genes, bacteria from the Ahringer collection were grown at 37°C for 8 hr in LB medium with 50 μg/mL carbenicillin and directly seeded onto NGM plates. 5 mM IPTG was used to induce dsRNA expression overnight at room temperature. All prepared plates were stored at 4°C till subsequent usage.

Cell lines

Mouse NIH/3T3 cells stably expressing dsRed2-fused mitochondrial targeting sequence (Mito-dsRed2) was a gift from the M. A. Frohman laboratory. The cells were cultured in Dulbecco's modified Eagle's Medium (Hylcone) supplemented with 10% Calf Serum (Hyclone) and maintained in 37°C with 5% CO_2.

METHOD DETAILS

Genomic screen

The *sqt-3(e2117)* temperature-sensitive mutant of *C. elegans* was utilized in the primary stage of the screening. These worms were kept at 15°C during embryonic and larval development, and assayed at 25°C as adults. The average time when their survival rate on *E. coli* BW25113 decreases to 10% was experimentally determined, which is on day-13 of adulthood. We used this time point to examine the survival of all the screening candidates. Positive hits with an increased survival rate were tested longitudinally first in the *sqt-3* mutant background, and then in wild-type worms (N2) at 20°C. Introduction of each candidate bacterial mutation into the parental strain as well as another *E. coli* strain MG1655 was performed, to confirm their lifespan-extending effects. The experimental design of the screen and the working flow are illustrated in Figure S1.

Bacterial growth and colonization analyses

For growth assay in liquid medium, bacteria of a single colony were inoculated in LB and grown at 37°C. OD_{600} was determined using LB medium as the blank control. For a plate assay, 30 μL of LB cultured bacteria at $OD_{600} = 0.4$ were seeded on each NGM plate, and were allowed to grow at 20°C. The bacteria were thoroughly washed off the plates with 1mL M9 buffer and OD_{600} was measured, with M9 buffer as the blank control.

For a viability assay, bacteria from seeded NGM plates (stored at 4°C) were washed off the plates with adequate M9 buffer till OD_{600} reaches below 0.1. The numbers of total bacterial cells were determined using a counting chamber (Hausser Scientific). The numbers of total live bacteria were determined based on colony forming unit on LB plates as described below. The percentage of living bacteria was then calculated.

To measure colonizing capacity of the bacteria in *C. elegans*, the nematodes were washed off the NGM plates at the selected age, and extensively rinsed with M9 buffer. The animals were then put on empty NGM plates with 100 μg/mL ampicillin for 1 hr. Using sterile techniques, 5 worms were individually picked into M9 buffer and homogenized. Part or all of the mixture was then plated onto LB plates. After incubated at 37°C overnight, the number of bacterial colonies were determined.

P1 phage transduction

Wild-type bacteriophage P1 was cultured overnight at 37°C together with the donor bacteria in 0.5 × LB agar to lysate the cells, and purification was done using 5% (v/v) chloroform. In case of taking a Keio mutant as the recipient cell, its kanamycin-resistant cassette was first removed using electro-transformation of plasmid pCP20 that contains the FLP recombinase. The phage lysate was incubated with the recipient cells at 32°C in LB medium containing 6mM sodium citrate before plated onto LB-citrate plates. The resulting mutants due to homologous recombination were obtained after sequential streaking on LB-citrate plates to remove phages, using kanamycin as a selection marker.

Restoration of lon functionality

For lifespan assays on OP50 expressing *lon*, the full-length *lon* gene was cloned into the plasmid pCA24N, which was used to transform *E. coli* OP50. The empty plasmid vector was used as the control. The successful insertion was confirmed by PCR. The resulting bacteria were cultured in LB medium at 37°C till the OD_{600} reached 0.6, and then seeded onto NGM plates with 1mM IPTG for induction. The plates were then incubated at 37°C for 24 hr before used for lifespan experiments.

Quantification of CA

Adapted methods were used to quantitatively compare CA production among bacterial strains (Dische and Shettles, 1948). For most *E. coli* strains, the bacteria was grown in M9 minimal medium at 37°C for 8 hr and at 20°C for 2 days. After centrifugation at 10,000 rpm for 20 min, the supernatant was considered as the assay sample. For the strains that cannot be grown in the M9 medium, including OP50 and a few auxotrophic Keio mutants, an alternative method was used to measure their secreted CA. In brief, the bacteria were cultivated in LB medium at 20°C overnight. After centrifugation to remove bacterial cells, the liquid medium was further centrifuged at 15,000 rpm for 30 min at 4°C. Equal volume of ethanol was then mixed with the supernatant, and put in 4°C overnight. Centrifugation was performed again to collect the pellet, which was then rinsed with cold 70% ethanol for 3 times and air-dried. The pellet from every 5 mL culture was dissolved in 1 mL ddH₂O as the assay sample. The assay samples were then quantified colormetrically. Briefly, 30 μL sample was mixed with 1 mL sulfuric/water solution (6:1 v/v) and boiled for 20 min. After cooling, the absorbance difference at 396nm and 430nm, $\Delta OD_{396-430}$, was measured using a spectrophotometer (BioTek). Cysteine hydrochloride was added to a final concentration of 3.5mg/mL, and $\Delta OD_{396-430}$ was measured again. The difference between these two values is proportional to the fucose concentration, and therefore the CA contents.

Purification and administration of CA

Adapted methods were used to purify CA polysaccharide from bacterial culture (Dische and Shettles, 1948). In brief, the **Δ***lon* mutant was grown in M9 minimal medium at 37°C overnight and at 20°C for 2 days. After heated in boiling water for 5 min, cells were removed by centrifugation and the supernatant was lyophilized. Every 5 mg of the resulting solid was dissolved in 1 mL water and centrifuged at 15,000 rpm for 20 min at 4°C. The supernatant was mixed with 1% (v/v) glacial acetic acid, boiled for 2 hr, and centrifuged at

15,000 rpm for 30 min at 4°C to precipitate lipopolysaccharides. The supernatant was then mixed with equal volume of chloroform/methanol (2:1 v/v) to eliminate proteins. 10K daltons dialysis cassettes (Thermo Scientific) were used to dialyze the aqueous phase against water at 4°C for 2 days. Solid CA was obtained after lyophilization, and sterilized under ultraviolet light for 2 hr. Purified CA was quantified as described above, after dissolved in water in a concentration of 1 mg/mL, with fucose solutions up to 100 µg/mL as standards.

For dietary supplementation of CA to worms, purified CA was dissolved in ddH$_2$O, and mixed with bacteria before seeding. Bacteria mixed with the same volume of ddH$_2$O were used as the vehicle control. For supplementation of CA to flies, highly concentrated CA solution was thoroughly mixed with fly cornmeal at 70°C. Same volume of ddH$_2$O were added as the vehicle control.

Lifespan and paralysis assays

Nematodes were age-synchronized as described above. Adults were kept separated from their offsprings by manually transferring to new rearing settings as necessary. Survival of the nematodes was examined on a daily basis. Death was scored by not responding to gentle mechanical prodding. Post-reproductive animals that are lost accidentally, dead of internal hatching or extruded organs were censored. The physical paralysis time of the Aß transgenic *C. elegans* was determined by observing their movement every day and analyzed in a similar manner. For lifespan analysis of the flies, animals were reared on the standard food till sexual segregation, and then were supplemented with CA, and kept transferred to new food every 4 days. Death was scored when a fly fails to move. Kaplan-Meier curves were analyzed using a Log-rank test.

Developmental time and brood size analyses

To determine the developmental time of *C. elegans*, 10 synchronized L1 worms were allowed to develop at 20°C. The animals were examined every 30 min to note their transition to L4, and the lapsed time from L1 to L4 was recorded for each individual. To assess the brood size, 10 synchronized L4 hermaphrodites were grown at 20°C, and kept transferred to fresh NGM plates every day. The number of progeny was counted until reproductive cessation, and the total number of progeny per individual was calculated. The experiments were performed for three times independently, and analyzed using a Student's t test.

Pharyngeal pumping, defecation cycle, and locomotion activity measurement

C. elegans on day-1 adulthood were monitored using an SMZ1500 stereo microscope (Nikon). The number of pharyngeal contractions in a single minute interval was counted. The time between the same phase of two consecutive defecations were also determined. Each randomly selected animal was measured for 3 times. The mean values of 10 animals were compared with the control using a Student's t test. A C11440 camera (Hamamatsu) connected to the microscope was used to record the spontaneous movement of the worms for one minute. Individual worms were tracked using NIS Elements AR imaging software (Nikon) and the average moving speed was calculated. Speeds of 20 animals were compared to the control using a Student's t test.

Gel permeation chromatography analysis

Gel permeation chromatography was performed using an Agilent 1260 Infinity chromatography system equipped with PLaquagel-OH Mixed (300 × 7.5 mm) and PL1120-6830 (300 × 7.5 mm) column set, 0.1 M NaNO$_3$ + 0.05% NaN$_3$ aqueous solution as eluent at 1.50 mL/min flow rate. Refractive index, right angle light scattering (RALS) and Low Angle Light Scattering (LALS) signals were acquired using Viscotek TDA 302 Triple Detection Array system. Both chromatography and the signal acquisition were performed at 40°C. Purified CA was dissolved in eluent at a concentration of 10.0 mg/mL and 100 µL of this solution were used for analysis. Signals were recorded and processed using a Malvern OmniSEC software. Assuming a typical dn/dc value of 0.147 for polysaccharides, the molecular weight of the purified CA was calculated.

Quantitative PCR analyses

For gene expression analysis, cDNA was synthesized using a Power SYBR Green Cells-to-Ct Kit (ThermoFisher Scientific) from lysate of 30 age-synchronized young adult worms. For mitochondrial content analysis, total DNA was released from worms lysed with proteinase K, followed by heat inactivation (Williams et al., 1992). Quantitative PCR was performed using a Kapa SYBR fast PCR kit (Kapa Biosystems) in an Eppendorf Realplex 4 PCR machine (Eppendorf). Values were normalized to those of *rpl-32* and *ant-1.3* as the internal control in gene expression and mitochondrial content analyses, respectively. All data shown represent three biologically independent samples. Statistical analysis was performed using a Student's t test.

ATP quantification

~3,000 age-synchronized worms were washed off the NGM plates as young adults, and extensively rinsed with M9 buffer to eliminate ingested bacteria. The worms were then sonicated in 500 µL 6M guanidine hydrochloride in extraction buffer (100mM Tris, 4mM EDTA, pH 7.8), flash frozen in liquid nitrogen, and heated in boiling water for 2 min. After cooling and centrifuged at 13,000 rpm for 5 min, the supernatant was diluted 1000 times with the extraction buffer. An ATP determination kit (Invitrogen) was used to quantify ATP in the samples, based requirement of luciferase for ATP in emitting light. With up to 1 µM ATP solutions provided by the manufacturer as the standards, the ATP concentration was determined using a luminometer (Berthold). The ATP contents were then

normalized to the total protein concentration, which was determined by a protein assay (Thermo Scientific). ATP was quantified in four independent samples, and compared between groups using a Student's t test.

Quantification of peptidase activities of the proteasome

~500 age-synchronized worms were washed off the NGM plates as young adults using M9 buffer. After rinsed with 1 mL washing buffer (50mM Tris-HCl, pH7.5, 250mM sucrose, 5mM MgCl$_2$) for 3 times and 500 μL lysis buffer (50mM Tris-HCl, pH7.5, 250mM sucrose, 5mM MgCl$_2$, 0.5mM EDTA, 2mM ATP, 1mM DTT) for 1 additional time, the worms were homogenized in 100 μL ice-cold lysis buffer. After centrifuged at 8,000 rpm for 15 min at 4°C, the protein content in the supernatant was determined using a protein assay (Thermo Scientific). The fluorogenic proteasomal substrates (Bachem) were diluted in assay buffer (50mM Tris-HCl, pH7.5, 40mM KCl, 5mM MgCl$_2$, 0.5mM ATP, 1mM DTT, 0.05mg/mL BSA): Suc-LLVY-AMC and Ac-RLR-AMC in 100 μM, while Ac-nLPnLD-AMC in 300 μM. 200 μL substrate was added into each well of a 96-well microtiter plate, together with lysate containing 50 μg total protein. After incubated at room temperature for 5 min, the fluorescence (excitation/emission: 380/460nm) was monitored using a fluorometer every 5 min for 1 hr. The slope representing relative proteasome activity was determined in three independent trials, and compared between groups using Student's t test.

Mitochondrial morphology assays and stimulated Raman scattering microscopy

Adult *C. elegans* at desired ages were individually picked into 0.1% sodium azide dropped on glass coverslips. The coverslips were then mounted onto pads of 2% agorose on microscope slides. Mouse NIH/3T3 cells stably expressing dsRed2-fused mitochondrial targeting sequence (dsRed2-Mito) were cultured in Dulbecco's modified Eagle's Medium (Hylcone) supplemented with 10% Calf Serum (Hyclone) and maintained in 37°C with 5% CO$_2$. Cells grown on glass coverslips were treated overnight with 0, 100, and 500 μg/mL of CA, respectively, and fixed with 4% paraformaldehyde in cytoskeleton stabilizing buffer (10mM PIPES, 150mM NaCl, 5mM EGTA, 5mM glucose, pH 6.8) for 10 min. Coverslips were washed with cytoskeleton stabilizing buffer for three times and mounted onto microscope slides using 4% n-propyl gallate. The slides were visualized under a confocal fluorescence microscope (Olympus) for mitochondrial morphology, or imaged under a Stimulated Raman Scattering (SRS) microscope (Ramachandran et al., 2015; Wang et al., 2011) for determining fat storage levels.

QUANTIFICATION AND STATISTICAL ANALYSIS

All the data were obtained from three or four biologically independent replicates. The Log-rank test (Kaplan-Meier survival method) was used to analyze lifespan and paralysis data. The non-parametric t test was used to analyze locomotion velocity. One-way ANOVA followed by Bonferroni's multiple comparison test was used to analyze CA levels in bacterial medium. For all the other quantifications, data were analyzed using a Student's t test. In all cases, p values < 0.05 was considered significant.
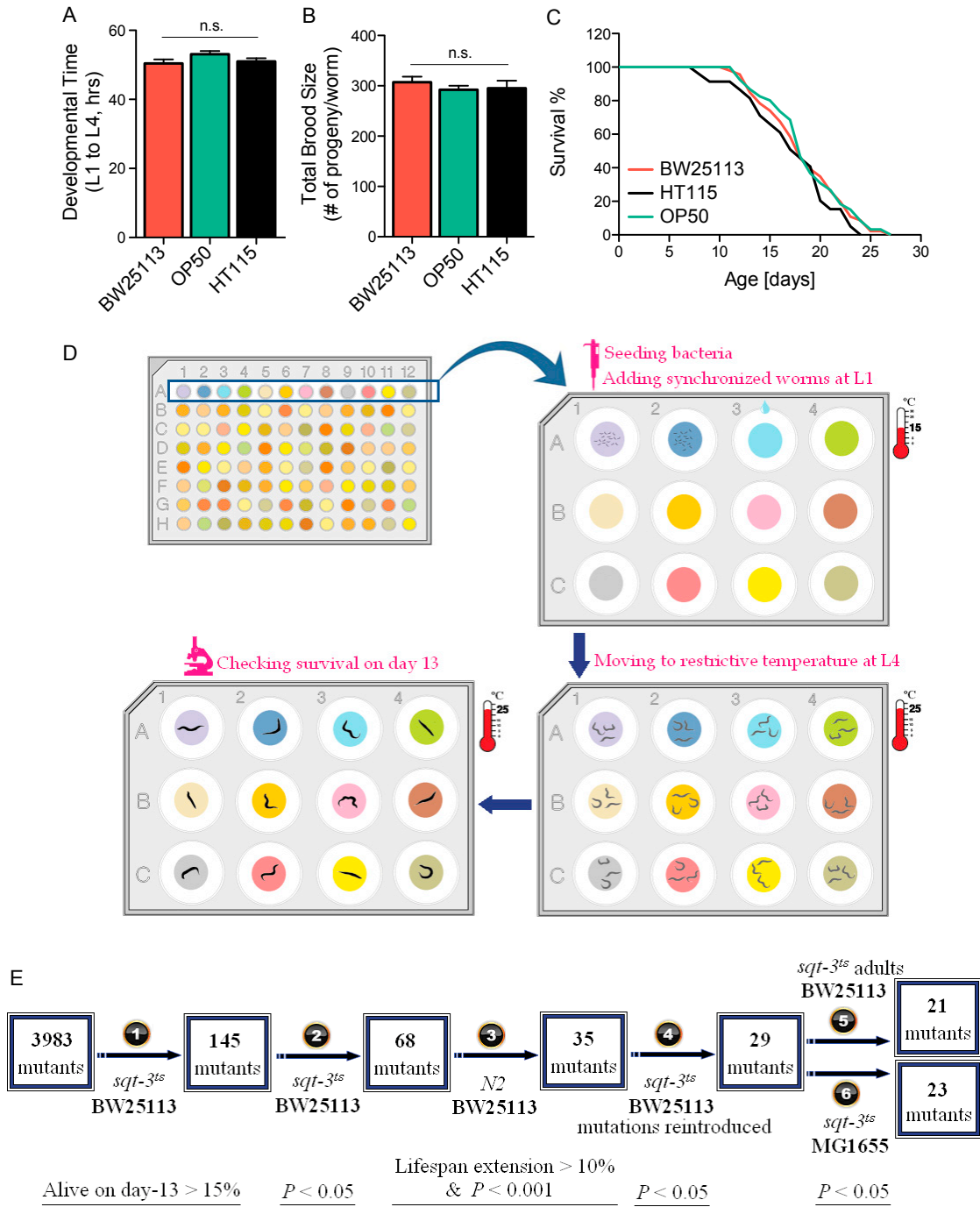
Figure S1. Characterization of Parental *E. coli* Strain and Experimental Design of Genetic Screens, Related to Figure 1

(A) Average times are 50.4 ± 1.2, 53.1 ± 0.9 and 51.2 ± 0.9 hr for wild-type (WT) L1 larvae developing into L4 larvae when grown on *E. coli* strains BW25113, OP50 and HT115, respectively. p > 0.05, Student's t test.

(B) Total numbers of progeny from WT adult worms grown on *E. coli* strains BW25113 (307 ± 11), OP50 (292 ± 8) and HT115 (295 ± 15) are not significantly different. p > 0.05, Student's t test.

(C) Lifespans of WT worms grown on *E. coli* strains BW25113, OP50, and HT115 are not significantly different (p > 0.05, Log-rank test). Mean lifespan of BW25113, 18.63 ± 0.31 days, n = 167; OP50, 19.32 ± 0.44 days, n = 121; HT115, 17.29 ± 0.96 days, n = 102.

(D) Schematic diagram of the procedures for the primary screen using the *sqt-3(e2117)^ts* collagen mutants, which are embryonic lethal at 25°C non-permissive temperature. Various light colors represent different bacterial mutants from the single-gene knockout *E. coli* library.

(E) The working flow of primary screens and subsequent retests. The entire process includes: (1) three rounds of primary screening; (2) further longitudinal confirmation; (3) validation of longevity in WT worms at 20°C with controlled bacteria amount; (4) validation of annotated bacterial mutations after reintroduction; (5) testing sufficiency upon adult-only supplementation; and (6) universality testing in another bacterial strain background. Boxes enclose the total numbers of mutants scored positive along the procedures. Utilized *C. elegans* strains, bacterial strains, and the criteria for positive hits are listed at each step.
Error bars represent standard error of the mean (SEM).
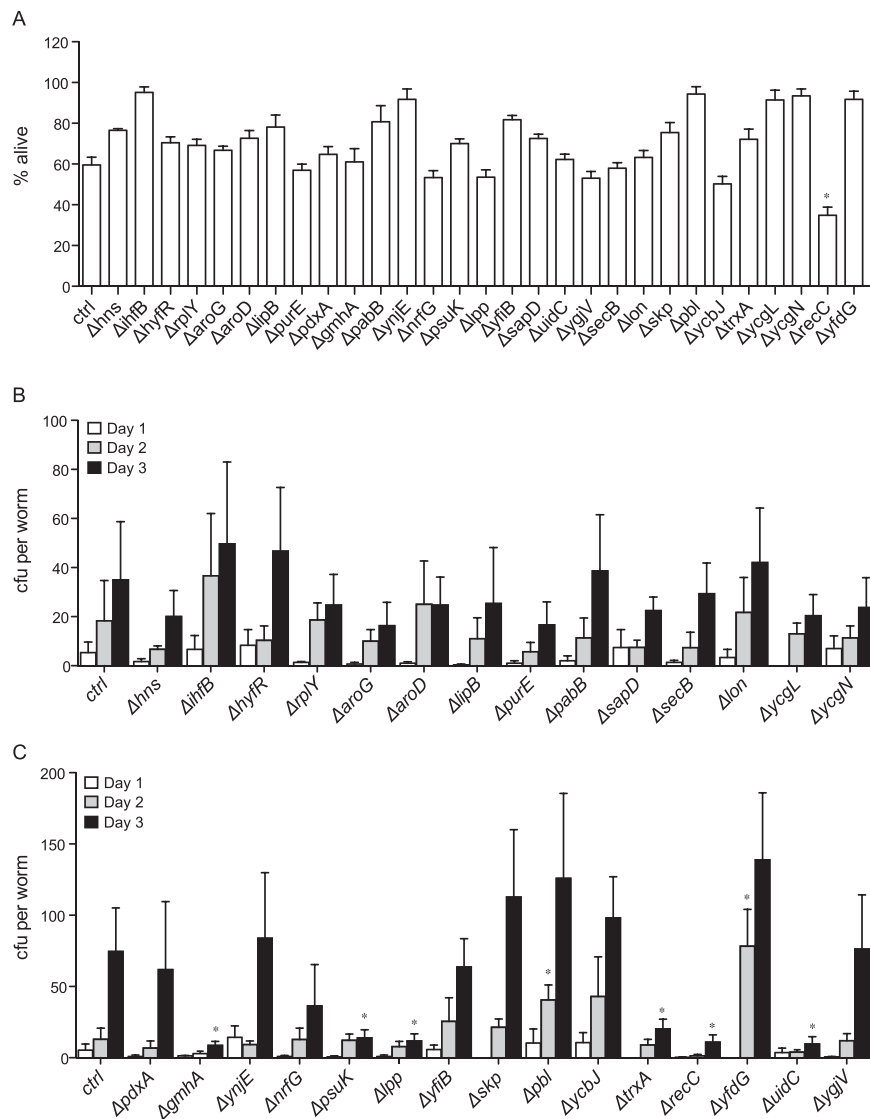
Figure S2. Viability and Host Colonization Capacity of the Longevity-Promoting Bacterial Mutants, Related to Figure 1

(A) Except *ΔrecC*, the bacterial mutants that prolong *C. elegans* lifespan do not exhibit decreased survival when provided to the host (p > 0.05, Student's t test).

(B and C) Longitudinal studies of colony forming in the WT *C. elegans* gut show limited alterations of colonization capacities by the pro-longevity bacterial mutations. Different degrees of shading delineate age of the *C. elegans*. *p < 0.05 compared to the control strain BW25113, Student's t test.

Error bars represent SEM.
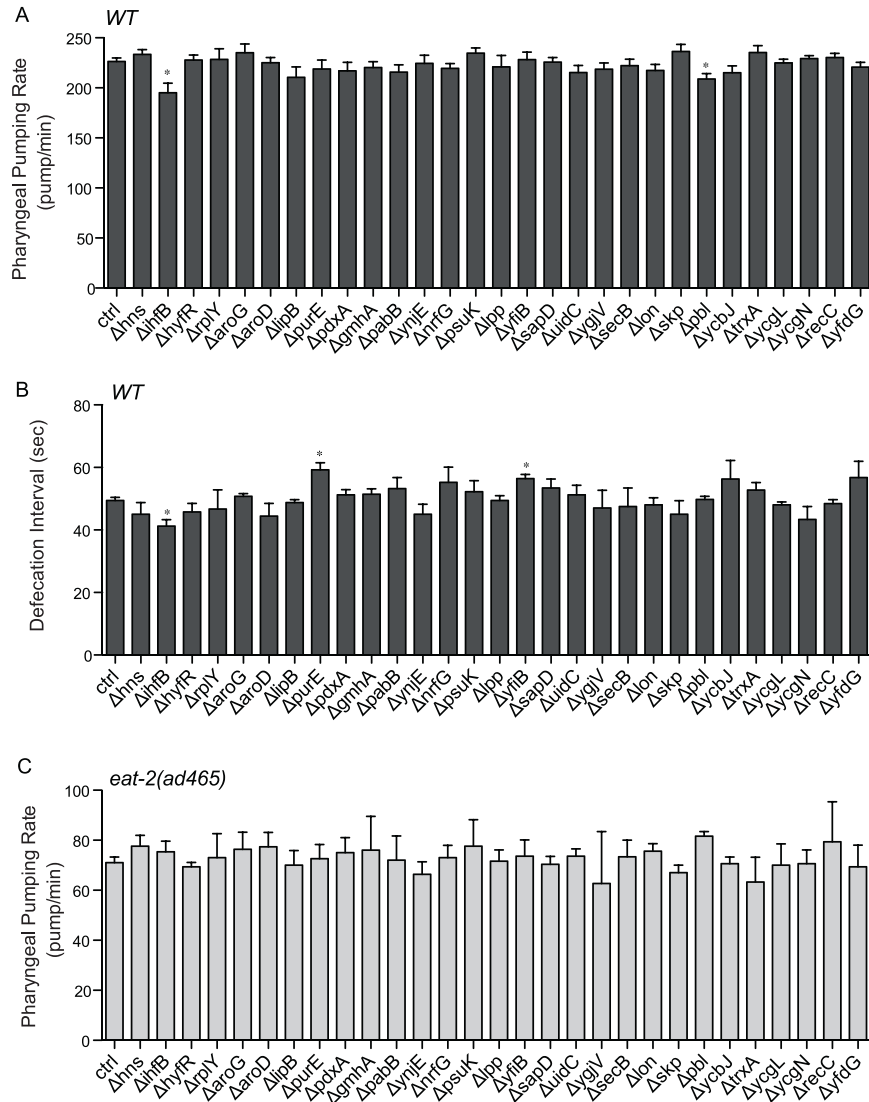
Figure S3. Effects of Longevity-Promoting Bacterial Mutants on *C. elegans* Feeding and Defecation Behaviors, Related to Figure 3

(A) Pharyngeal pumping rates were measured in day-1-old WT worms grown on the bacterial mutants that prolong lifespan.

(B) Defecation interval length was examined in day-1-old WT worms grown on the bacterial mutants that prolong lifespan.

(C) Pharyngeal pumping rates were measured in day-1-old *eat-2(ad465)* mutants grown on the bacterial mutants that prolong lifespan.

*p < *0.05* compared to the control, Student's t test; error bars represent SEM.
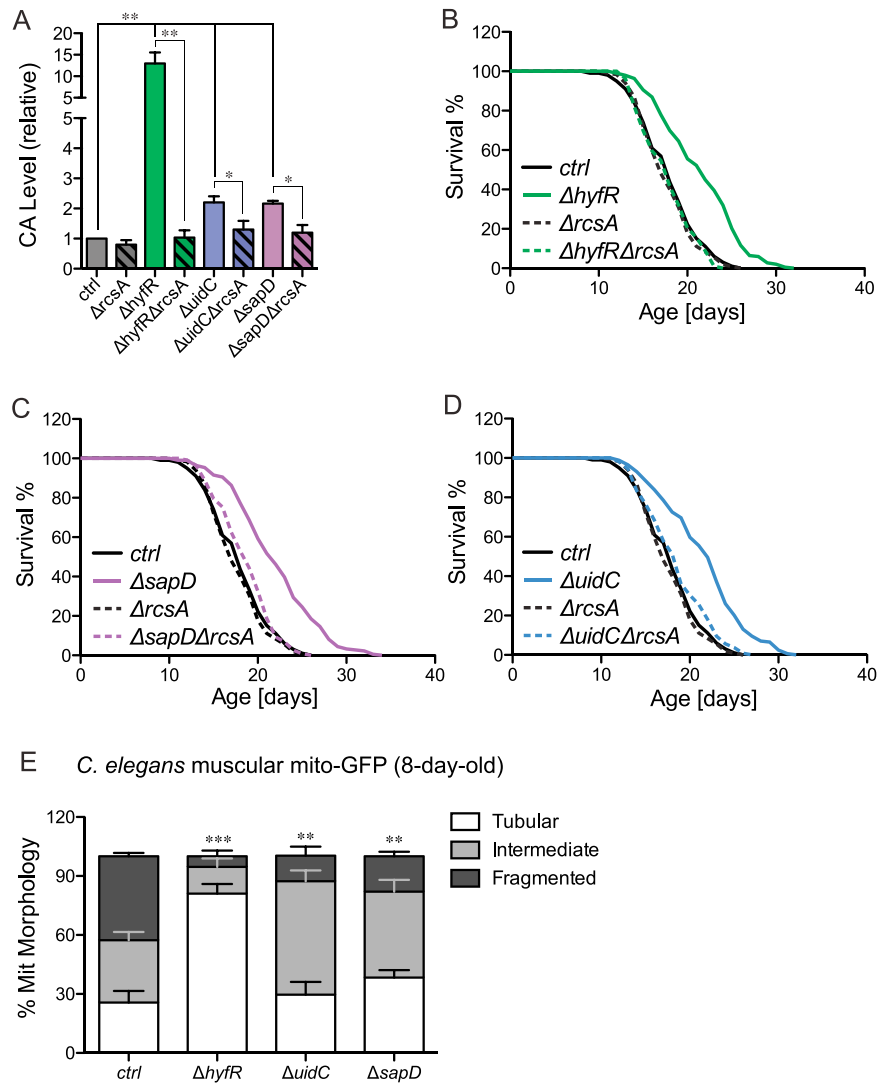
Figure S4. RcsA-Dependent CA Production and Beneficial Effects Conferred by Three Bacterial Mutants, Related to Figure 4

(A) CA production is elevated in three bacterial mutants: *ΔhyfR*, *ΔuidC* and *ΔsapD* (**$p < 0.01$, *$p < 0.05$, one-way ANOVA compared to the parental control followed by Bonferroni's multiple comparison test).

(B–D) The deletion mutation of *ΔrcsA* abrogates host longevity conferred by *ΔhyfR* (B), *ΔsapD* (C), and *ΔuidC* (D) ($p > 0.05$, *ΔrcsA* versus the double mutants, Log-rank test). Experiments were conducted in parallel with same parental controls and *ΔrcsA* mutants.

(E) The CA-overproducing mutants of *ΔhyfR*, *ΔuidC* and *ΔsapD* all significantly lower the levels of age-associated muscular mitochondrial fragmentation in the transgenic *C. elegans* line *(raxIs[myo-3p::mitoGFP])* (**$p < 0.01$ compared to the parental control, Student's t test).
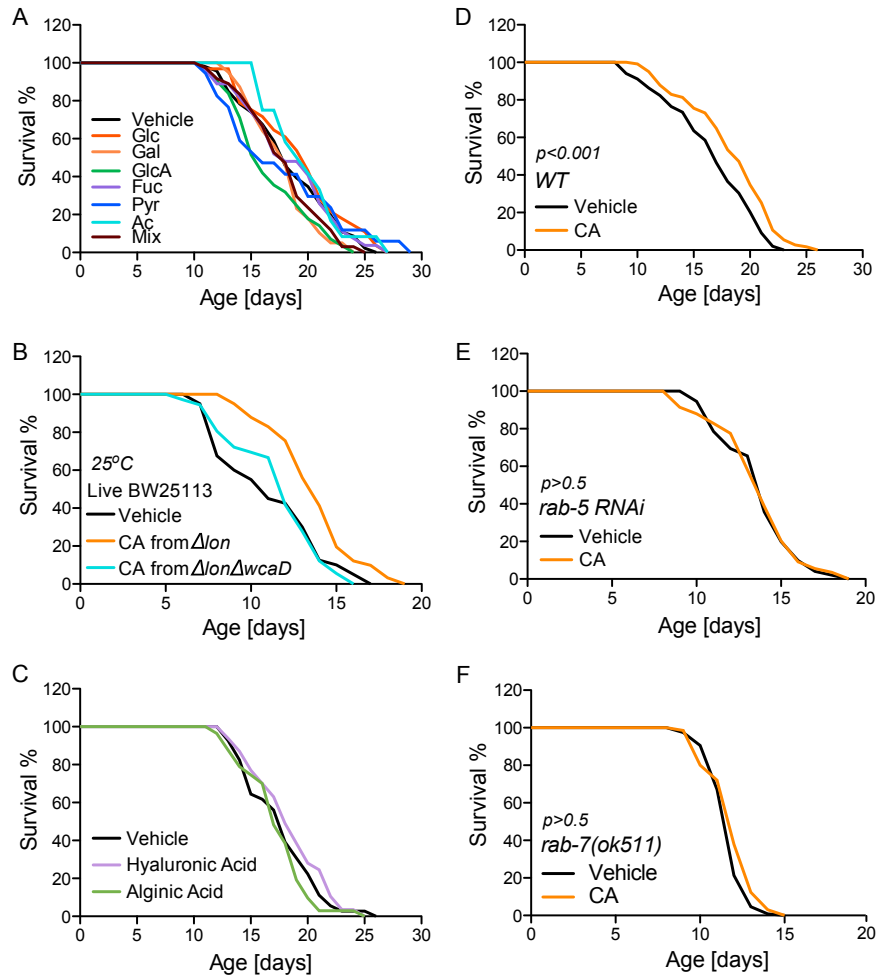
Error bars represent SEM.

Figure S5. Lifespan Effects of CA Monomers and Other Polysaccharides and the Requirement of Host Endocytosis for CA-Induced Longevity, Related to Figure 6

(A) Supplementation with CA monomers does not extend *C. elegans* lifespan (p > *0.1*, Log-rank test). Glc, glucose; Gal, galactose; Fuc, fucose; GlcA, glucuronic acid; Pyr, sodium pyruvate; Ac, acetic acid; Mix, the combination of all these monomers.

(B) Extracts were purified from the *Δlon* and the *ΔlonΔwcaD* bacterial mutants in parallel. Supplementation of *Δlon* extracts extends the lifespan of *C. elegans* by 15% (p < *0.001*, Log-rank test), while extracts from the *ΔlonΔwcaD* double mutant do not significantly affect *C. elegans* lifespan (p > *0.5*, Log-rank test).

(C) Supplementation with other polysaccharides—hyaluronic acid (HA) and alginic acid (AA)—does not extend the lifespan of *C. elegans* (p > *0.1*, Log-rank test).

(D–F) CA supplementation prolongs lifespan of WT *C. elegans* (D), but is failed to do so with inactivation of either *rab-5* (E) or *rab-7* (F) that blocks early endosome to late endosome or late endosome to lysosome fusion, respectively. p > *0.5*, CA versus vehicle control, Log-rank test.
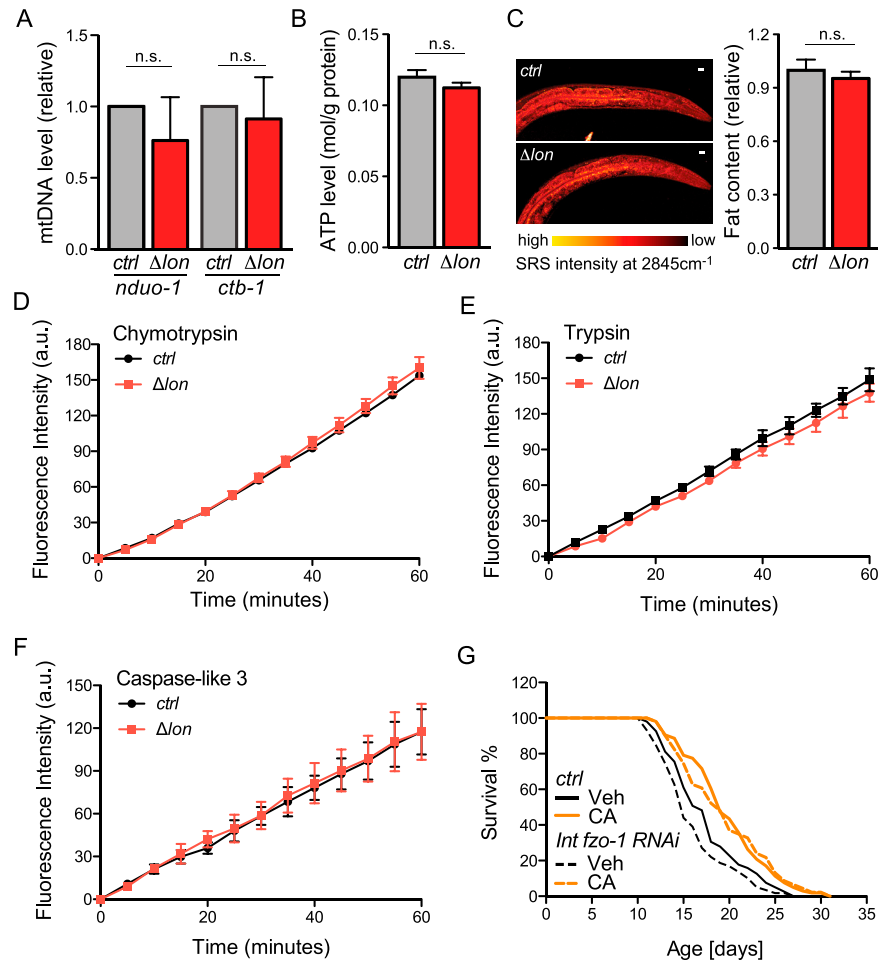
Figure S6. Effects of CA Overproduction on *C. elegans* Mitochondria and Proteasome, Related to Figure 7

(A) Mitochondrial DNA amounts assessed using two mitochondrial genome-encoded genes, *nduo-1* and *ctb-1* show no difference between *C. elegans* on the parental control and *Δlon* mutant bacteria. Error bars represent standard deviation (s.d.), $p > 0.05$, Student's t test.

(B) *C. elegans* on the parental control and *Δlon* mutant bacteria have similar levels of ATP. Error bars represent s.d., $p > 0.05$, Student's t test.

(C) Total fat levels stored in the intestine were measured by stimulated Raman scattering (SRS) microscopy, and are similar between *C. elegans* on the parental control and *Δlon* mutant bacteria. Error bars represent s.d., $p > 0.05$, Student's t test.

(D–F) CA supplementation does not affect *C. elegans* proteasome functions assayed by chymotrypsin (D), trypsin (E) and caspase-like 3 (F) activities.

(G) Intestinal-specific knockdown of *fzo-1* by RNAi does not affect the lifespan-extending effect of CA. $p < 0.001$, CA versus vehicle control (*fzo-1* RNAi), Log-rank test.
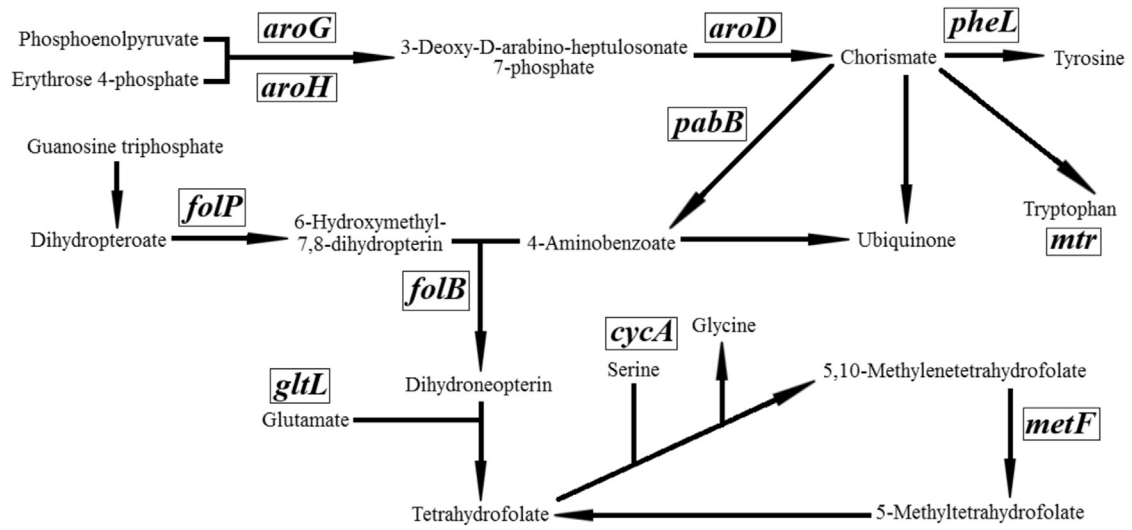
Figure S7. A Group of Longevity-Promoting *E. coli* Mutants Are Involved in the Biosynthesis Pathway of Chorismate and Its Derivatives, Related to Figure 1